A systematic assessment of uncertainties in large scale soil loss estimation from different representations of USLE input factors - A case study for Kenya and Uganda

Christoph Schürz[1], Bano Mehdi[1,2], Jens Kiesel[3,4], Karsten Schulz[1], and Mathew Herrnegger[1]

[1]Institute for Hydrology and Water Management, University of Natural Resources and Life Sciences, Vienna (BOKU), Vienna, Austria
[2]Institute of Agronomy, University of Natural Resources and Life Sciences, Vienna (BOKU), Tulln, Austria
[3]Leibniz Institute of Freshwater Ecology and Inland Fisheries (IGB), Berlin, Germany
[4]Institute of Natural Resource Conservation, Department of Hydrology and Water Resources Management, Christian Albrechts University of Kiel, Kiel, Germany

Correspondence: Christoph Schürz (christoph.schuerz@boku.ac.at); Mathew Herrnegger (mathew.herrnegger@boku.ac.at)

Abstract. The Universal Soil Loss Equation (USLE) is the most commonly used model to assess soil erosion by water. The model equation quantifies long-term average annual soil loss as a product of the rainfall erosivity R, soil erodibility K, slope length and steepness LS, soil cover C and support measures P. A large variety of methods exist to derive these model inputs from readily available data. However, the estimated values of a respective model input can strongly differ when employing

5   different methods and can eventually introduce large uncertainties in the estimated soil loss. The potential to evaluate soil loss estimates at a large scale are very limited, due to scarce in-field observations and their comparability to long-term soil estimates. In this work we addressed (i) the uncertainties in the soil loss estimates that can potentially be introduced by different representations of the USLE input factors and (ii) challanges that can arise in the evaluation of uncertain soil loss estimates with observed data.

10   In a systematic analysis we developed different representations of USLE inputs for the study domain of Kenya and Uganda. All combinations of the generated USLE inputs resulted in 756 USLE model setups. We assessed the resulting distributions in soil loss, both spatially distributed and on the administrative level for Kenya and Uganda. In a sensitivity analysis we analyzed the contributions of the USLE model inputs to the ranges in soil loss and analyzed their spatial patterns. We compared the calculated USLE ensemble soil estimates to available in-field data and other study results and addressed possibilities and

15   limitations of the USLE model evaluation.

    The USLE model ensemble resulted in wide ranges of estimated soil loss, exceeding the mean soil loss by over an order of magnitude particularly in hilly topographies. The study implies that a soil loss assessment with the USLE is highly uncertain and strongly depends on the realizations of the model input factors. The employed sensitivity analysis enabled us to identify spatial patterns in the importance of the USLE input factors. The C and K factors showed large scale patterns of importance

20   in the densely vegetated part of Uganda and the dry north of Kenya, respectively, while LS was relevant in small scale heterogeneous patterns. Major challenges for the evaluation of the estimated soil losses with in-field data were due to spatial and

temporal limitations of the observation data, but also due to measured soil losses describing processes that are different to the ones that are represented by the USLE.

1 Introduction

The Universal Soil Loss Equation (USLE, Wischmeier and Smith, 1965, 1987) formulates the most commonly applied concept
5 to assess soil loss by water erosion (Alewell et al., 2019; Borrelli et al., 2017; Panagos et al., 2015e; Kinnell, 2010). The USLE is an empirical relationship that computes long-term average annual soil loss as a product of six input factors that characterize the erosive forces of the rainfall (R), the soil erodibility (K), topography (L and S), plant cover (C), and support practices to mitigate erosion (P). Historically, the USLE succeeded earlier attempts to quantify soil erosion by water developed for the Corn Belt region of the United States of America (USA) in the 1940s. First relationships between soil loss on cropland and
10 topography (Zingg, 1940), factors for crops and conservation practices (Smith, 1941), soil erodibility (Browning et al., 1947), and rainfall (Musgrave, 1947) were developed and reported by Wischmeier and Smith (1965). Over several decades extensive soil erosion data were collected in many locations on field plot scale in the USA. Eventually more than 10000 plot-years of field data were analyzed with reference to a "unit plot" to formulate a generally applicable approach for soil loss estimation in the USA (Wischmeier and Smith, 1965; Kinnell, 2010; Renard et al., 2011). The new approach overcame restrictions of previous
15 methods for soil loss estimation to specific regions in the USA and thus was termed "universal" in the literature (Wischmeier and Smith, 1965). Further data were collected over the following decades and the methods to calculate the USLE input factors were substantially revised (Renard et al., 1991, 1997; Govers, 2011). The revised model was termed as the Revised USLE (RUSLE, Renard et al., 1991). Yet, the general structure of the equation remained unchanged.

In the following we refer to USLE or RUSLE type models as USLE for simplicity. The different revisions of the USLE were
20 summarized in Agriculture Handbooks (Wischmeier and Smith, 1965, 1987; Renard et al., 1997) that proved to be pragmatic and effective tools for soil conservation planning in the USA (Renard et al., 1991, 2011). Not without causing controversies, applications of the USLE model were extended to other land uses than cropland (Renard et al., 1991; Alewell et al., 2019), such as rangeland (Spaeth et al., 2003; Weltz et al., 1998), or woodland (Dissmeyer and Foster, 1980). Due to the principally simple implementation of the USLE model it found a wide application outside of the USA in more than 100 countries (Alewell
25 et al., 2019) at various spatial scales and in various geoclimatic regions (Benavidez et al., 2018). Several studies adopted the methods to calculate the USLE input factors to meet local or regional conditions (e.g., Roose, 1975; Moore, 1979; Bollinnne, 1985; Favis-Mortlock, 1998; Angima et al., 2003). Yet, to coin this empirical relationship as being "universal" is misleading for applications outside the USA and to non cropland (Jetten and Favis-Mortlock, 2006). The application of the USLE to conditions different from the plot experiments must be treated as a model extrapolation that is not supported by field data
30 (Bosco et al., 2015; Favis-Mortlock, 1998).

It is well accepted that the USLE does not at all attempt to represent the physical processes to erode and transport soil particles, but rather empirically relates field properties to long term soil loss (Beven and Brazier, 2011; Kinnell, 2010). The USLEs' wide application does not distinguish it to be the best, or only option for soil loss estimation (Evans and Boardman,

2016a). Limitations of the USLE (but also other soil erosion models) have been well documented in the literature (see e.g. Boardman, 1996, 2006). Jetten and Favis-Mortlock (2006) summarize applications of the USLE in Europe, where the validation of calculated soil losses with observed data showed poor results (e.g., Favis-Mortlock, 1998; Bollinnne, 1985). Kinnell (2010) reports a good performance of a locally adapted variant of the USLE in New South Wales, Australia, but documents the

5 over-prediction of small soil losses and under-prediction of large soil losses when applied to larger domains with a higher variability in agricultural systems (Tiwari et al., 2000; Risse et al., 1993). A recent pan-European soil loss assessment started a broad discussion of the validity of the estimates when compared to in-field soil loss assessments in Great Britain (see the discussion in Panagos et al., 2015e; Evans and Boardman, 2016a; Panagos et al., 2016; Evans and Boardman, 2016b). Several authors question the applicability of the plot scale based USLE to the landscape scale (e.g., Boardman, 2006; Evans, 1995;

10 Govers, 2011), particularly as in large domains other processes such as gully erosion, bank erosion, or sediment deposition can dominate the erosion response (Govers, 2011). Evans (2013) concludes that the USLE can be helpful to identify the erosion potential or erosion hot spots, but fails to predict the exact magnitude of erosion.

The above criticism does not impede the wide application of the USLE. For large scale erosion assessments, the availability of large scale spatial data and methods to the infer the USLE inputs facilitate its implementation in GIS (Govers, 2011) and

15 therefore is an attractive option to assess soil erosion. The implementation of remote sensing (satellite) products advances large scale soil loss assessments, particularly in data scarce regions where observations are limited as well as in large domains where in-field data acquisition is infeasible (Alewell et al., 2019; Bosco et al., 2015). This procedure yielded several continental and global estimates of USLE input factors (e.g., Panagos et al., 2017, 2015a, b, c; Vrieling et al., 2010) and soil loss assessments (e.g., Borrelli et al., 2017; Panagos et al., 2015e; Naipal et al., 2015; Yang et al., 2003; Van der Knijff et al., 2000) that were

20 primarily derived from large scale (remote sensing) data products. The methods to compute realizations for the USLE inputs that were proposed in these (and other) large scale assessments attempt to employ data products that describe (or are a proxy for) features in the landscape (such as topography, or vegetation cover) to infer spatially distributed estimates for the USLE inputs. For each USLE input, various methods exist to generate the spatially distributed estimates for the USLE inputs that use different data sources (see e.g. the review of Benavidez et al., 2018). Thus, differing results in the realizations of a USLE

25 input factor can follow from the different computational approaches. However, a typical setup of the USLE combines only one representation of each USLE input in a single model setup and therefore does not depict the variations in the soil loss calculations that may arise from different representations of the USLE input factors. Very few studies consider the impact of the different representations of the ULSE inputs (e.g., Bosco et al., 2015) to account for the resulting ranges in calculated soil loss. Because of the multiplicative structure of the USLE, uncertainties in the input factors are decisive for the computation of

30 the soil loss as they are also propagated by multiplication.

A widely applied procedure in environmental modelling to gain confidence in a model setup is model validation, which is the evaluation of calculated model outputs against observed data (Beven and Young, 2013; Young, 2001). Beven and Young (2013) further stress the importance of model falsification when a model fails to reproduce observations. For large scale soil loss assessments the possibilities to evaluate calculated soil losses, or spatially distributed estimates of the USLE inputs are

35 very limited (Bosco et al., 2015; Van der Knijff et al., 2000). Typically, studies that monitored soil loss within the study domain

rarely exist. Existing in-field data, however, entail issues of their spatial and temporal representativeness (Evans, 2013; Govers, 2011). Boardman (2006) questions the comparability of erosion plot data or in-stream sediment yields with soil losses at the catchment scale. Govers (2011) highlights that USLE estimates reflect long time periods (Wischmeier and Smith (1965) e.g. recommended 20 years). Such time periods are usually not covered by a soil loss monitoring campaign. Eventually, USLE

5 input factor estimates and large scale soil loss assessments are compared to very limited observation data (e.g., Borrelli et al., 2017; Vrieling et al., 2010; Moore, 1979) and in many cases no validation was carried out at all (e.g., Karamage et al., 2017; Van der Knijff et al., 2000).

Acknowledging that soil loss assessments using the USLE is uncertain and that the evaluation of soil loss estimates in large scale assessments has limitations, we formulate and systematically address the following objectives:

10   i. What are the uncertainties in soil loss estimates that we can expect from the implementation of different model input realizations in the USLE model? How can we interpret uncertain soil loss estimates?

    ii. Which USLE model inputs contribute the most to the uncertainties of the soil loss estimates?

    iii. Can we we compare the calculated soil loss estimates to in-field soil loss data? Does the evaluation enable us to reduce the uncertainties in the estimated soil losses?

15   We addressed these questions in a large scale soil loss assessment for Kenya and Uganda and structured our work in the following way: We reviewed methods to calculate USLE inputs that were widely used in previous large scale soil loss assessments and employed selected methods to generate spatially distributed estimates for the study domain (see section 3.2). All combinations of the input factor realizations delineate a USLE model ensemble. The analysis of the USLE ensemble results is outlined in the sections 3.4, 4.1, and 5.1. We analyzed the impact of the USLE input factors R, LS, K, and C on the calculated

20 ranges of the soil loss estimates in a spatial analysis (see sections 3.5, 4.2, and 5.1). For selected erosion prone counties of Kenya and districts of Uganda, we analyze the spatially aggregated mean soil loss estimates and compare them to the results on the administrative level for Uganda in Karamage et al. (2017) (sections 4.3 and 5.1). In a final step we selected in-field erosion studies that were conducted in Kenya and Uganda and compare the reported in-field erosion data to the ensemble soil loss estimates derived with the USLE model ensemble (sections 4.4 and 5.2)

2   Study Area

The study area covers the countries of Kenya and Uganda, located in East Africa (Fig. 1). Overall the Sub-Saharan countries experienced drastic land degradation and a decrease in net-primary productivity of the land over the last decades (Bai et al., 2008). The dominant driver for land degradation in the horn of Africa is soil erosion by water (Jones et al., 2013). Large parts of Kenya and Uganda are generally prone to soil loss by water induced erosion.

30   In total, the study region covers an area of 821405 km^2, of which 729622 km^2 or 89 % of the surface are analyzed, since lakes and other water bodies are excluded from the analysis. Additionally, 27 administrative units in both countries (Fig. 1a),
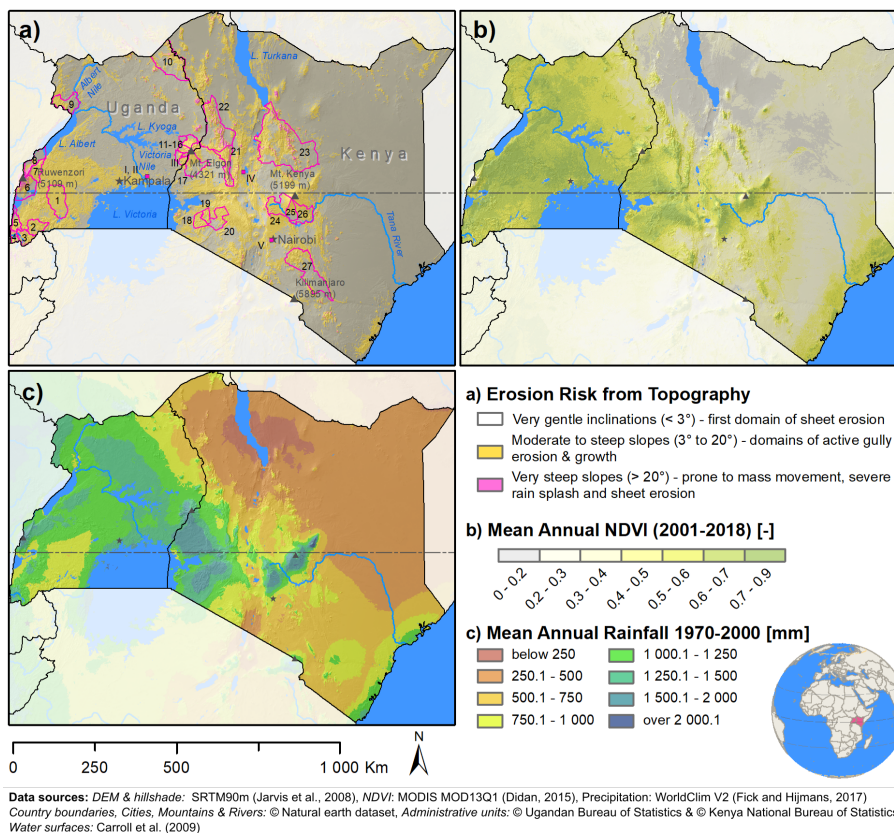
Figure 1. Study area covering the countries of Kenya and Uganda. A classification of the soil erosion risk after Ebisemiju (1988) (a), the mean annual MODIS NDVI as a proxy for vegetation cover (b), and mean annual rainfall (c) are plotted to characterize spatial properties of the study region. The boundaries for administrative units where the mean soil loss was assessed are shown with pink outlines in panel a). Locations of soil loss assessments from previous studies that were used for comparison are shown as pink squares.

Table 1) are analysed in detail. The selection of the erosion prone administrative units is based on a visual analysis of Fig. 1a) and on local knowledge and on-site experience.

The study region covers a wide range of factors influencing soil erosion. Fig. 1a) shows the potential erosion risk solely
5   stemming from topography, based on thresholds by Ebisemiju (1988). Large areas with moderate to steep slopes ("moderate risk") are evident in the South-West of Uganda and in a north-to-south band in Kenya, where the Western or Gregory Rift as part of the Great Rift Valley transects the country. The area in Uganda is characterized by a hilly topography with low elevation differences. In contrast, the erosion prone regions in Kenya are mostly characterized by larger elevation differences, e.g. escarpments. Very steep slopes that exhibit a high risk of erosion from topography are evident around mountain massifs, e.g. Ruwenzori (5109 m a.s.l., Uganda), Mt. Elgon (4321 m a.s.l., Uganda and Kenya) or Mt. Kenya (5199 m a.s.l., Kenya).
10   Additionally, high erosion risk prone areas are evident in the south-western corner of Uganda and along the Rift Valley in the northern part of Kenya. Fig. 1b) shows the mean annual MODIS NDVI (Didan, 2015) for the period 2001 - 2018 as a proxy

Table 1. Administrative units analysed in more detail. The locations are shown in Fig. 1a). The slope and elevation statistics are based on SRTM v4.1 90m DEM (Jarvis et al., 2008).

Nr.	Country	Greater Region	Administrative unit	Area (km^2)	Mean slope (deg)	Max. slope (deg)	Mean elev. (m)	Max. elev. (m)	Min. elev. (m)
1	Uganda	-	Kiruhura	4636	4.39	28.96	1310	1670	1178
2	Uganda	Lake Bunyoni	Ntungamo	2062	7.57	43.61	1497	2224	1279
3	Uganda	Lake Bunyoni	Kabale	1740	14.79	46.15	1990	2601	1355
4	Uganda	Lake Bunyoni	Kisoro	733	11.95	49.44	1983	3861	1338
5	Uganda	Lake Bunyoni	Kanungu	1335	8.61	46.52	1388	2499	912
6	Uganda	Ruwenzori	Kasese	3402	8.81	60.54	1493	5034	878
7	Uganda	Ruwenzori	Kabarole	1825	8.01	48.94	1515	3996	626
8	Uganda	Ruwenzori	Bundibugyo	2265	5.65	52.24	1002	4659	612
9	Uganda	-	Nebbi	2922	3.71	34.70	1039	1873	612
10	Uganda	-	Kaabong	7301	5.87	61.41	1416	2720	834
11	Uganda	Mt. Elgon	Bukwo	529	12.28	53.35	2420	4204	1253
12	Uganda	Mt. Elgon	Kapchorwa	1215	8.00	53.39	1823	4265	1062
13	Uganda	Mt. Elgon	Sironko	1106	7.15	60.43	1619	4280	1045
14	Uganda	Mt. Elgon	Bududa	253	16.99	61.70	2103	4314	1216
15	Uganda	Mt. Elgon	Mbale	522	5.50	71.23	1288	2351	1083
16	Uganda	Mt. Elgon	Manafwa	606	8.34	57.77	1608	3319	1139
17	Kenya	Mt. Elgon	Bungoma	3036	5.15	45.12	1859	4304	1213
18	Kenya	S-W Kenya	Kisii	1353	6.24	32.83	1750	2190	1394
19	Kenya	S-W Kenya	Nyamira	897	6.70	31.99	1888	2214	1509
20	Kenya	S-W Kenya	Bomet	2384	5.14	30.29	1997	2465	1693
21	Kenya	Cherangani Hills	Elgeyo-Marakwet	3058	9.97	60.70	2122	3517	920
22	Kenya	Cherangani Hills	West Pokot	9328	8.70	67.15	1443	3524	691
23	Kenya	-	Samburu	21250	6.81	66.83	1185	2834	296
24	Kenya	Mt. Kenya	Nyeri	3380	7.39	54.88	2284	5035	1210
25	Kenya	Mt. Kenya	Kirinyaga	1491	4.41	45.27	1619	4747	1057
26	Kenya	Mt. Kenya	Embu	2780	4.89	38.56	1191	4760	520
27	Kenya	-	Makueni	8297	3.84	58.42	1065	2120	404

for the vegetation cover. Higher values in NDVI show pixels with high vegetation cover, where a lower risk of water erosion due to ground cover can be assumed, and vice-versa. Kenya exhibits a large variability in NDVI with low values in the arid to semi-arid northern and south-eastern parts. Higher vegetation cover is present at the coast towards the Indian Ocean, around Mt. Kenya, but also around Lake Victoria in the western part of the country. Uganda shows a rather homogeneous vegetation

5   distribution, with some semi-arid areas in the north-east showing a lower vegetation cover.

Fig. 1c) shows the long-term mean annual rainfall (based on WorldClim Version2 for the period 1970 – 2000, Fick and Hijmans, 2017) as a proxy for the erosivity by rainfall. This assumes that larger annual rainfall values lead to higher erosion rates. Rainfall and vegetation cover are clearly connected. Hence, a more homogeneous rainfall pattern is visible for Uganda. Dryer areas in the south-west and north-east receive around $750 – 1000 \, \mathrm{mm \, yr^{-1}}$ of precipitation. The center of the country is

10   wetter with around $1000 – 1500 \, \mathrm{mm \, yr^{-1}}$. In Kenya, wetter areas are evident around Lake Victoria and Mt. Kenya, receiving $1500 – 2000 \, \mathrm{mm \, yr^{-1}}$ or even higher. The northern part of the country only receives $250 – 500 \, \mathrm{mm \, yr^{-1}}$. Here, areas around Lake Turkana are very dry, with an annual precipitation of less than $250 \, \mathrm{mm \, yr^{-1}}$. In accordance with vegetation cover, the coast is wetter ($1000 – 1250 \, \mathrm{mm \, yr^{-1}}$). Between the coast and the central highlands, a dry belt is visible ($500 – 750 \, \mathrm{mm}$ $\mathrm{yr^{-1}}$).

15   ## 3   Methods and Data Basis

3.1   The Universal Soil Loss Equation (USLE)

The general form of USLE-type equation is as follows:

$$A = R \times K \times LS \times C \times P \tag{1}$$

where A is the long-term average annual soil loss in $\mathrm{tons \, ha^{-1} \, yr^{-1}}$, R is the rainfall erosivity in $\mathrm{MJ \, mm \, ha^{-1} \, h^{-1} \, yr^{-1}}$,

20   K is the soil erodibility factor in $\mathrm{tons \, h \, MJ^{-1} \, mm^{-1}}$, L and S are the unitless slope length factor and the slope steepness factor (that are usually evaluated together as the topographic factor LS (Renard et al., 1997)), C is the unitless cover management factor, and P is the unitless support practice factor.

3.2   Estimation of USLE model inputs

To address the impact of different USLE input factor realizations on the simulation of the soil loss A, we generated a set of

25   realizations for each of the four USLE input factors R, K, LS, and C. Methods to calculate the inputs were considered that were either used in previous large scale applications or that were specifically developed for Eastern Africa (or regions with similar climatic, topographic, and vegetation conditions). The implemented methods are described below. Further details to the input factor generation is provided in the supplementary materials section S.1. The support practice factor P was excluded from the analysis, as large scale data to derive estimates for P are very limited. Previous large scale studies, for example,

inferred the P factor from relationships with the land use (e.g., Yang et al., 2003), or implemented a global estimate of P for the entire study region (e.g., Karamage et al., 2017), or did not consider the P factor (e.g., Borrelli et al., 2017).

The rainfall erosivity factor R relates the intensity of rainfall events to the kinetic energy that is available to erode soil particles (Wischmeier and Smith, 1987; Panagos et al., 2015a). Rainfall intensity records are hardly available for large domains.
5   Thus, large scale erosion studies often employ long-term annual average precipitation sums to infer R. We implemented long-term monthly precipitation provided by WorldClim Version2 (Fick and Hijmans, 2017) with a spatial resolution of 30 seconds and aggregated the monthly values to annual precipitation. We considered the following five methods that relate long-term mean annual precipitation (P_{annual}) to R, but differ in their type of mathematical relationship (Fig. 2a)). Roose (1975) and Moore (1979) developed relationships between mean annual rainfall sums and R based on station data in Western and Eastern
10 Africa, respectively. Karamage et al. (2017) used the method developed by Lo et al. (1985) to calculate R for Uganda. The method of Renard and Freimund (1994) was developed for USA precipitation station data and has been employed in global applications (e.g., Naipal et al., 2015; Yang et al., 2003). Nakil (2014) developed a relationship between precipitation and R for the highly variable rainfall patterns of the west coast of India. Additionally, we considered recent products by Panagos et al. (2017) and Vrieling et al. (2014) that inferred R estimates from high temporal precipitation data. While Panagos et al. (2017)
15 derived global estimates for R on a 1km grid based on a large global rainfall intensity data set to assemble the GloREDa data base, Vrieling et al. (2014) used the 3 hourly TRMM Multi-satellite Precipitation Analysis (TMPA) product (Huffman et al., 2007) to infer R estimates for the African continent in a 0.25° spatial resolution. In total we included seven realizations for R in this study (Fig. 2 a)).

The soil erodibility factor K describes the tendency of a soil to erode due to the erosive force of precipitation or surface runoff
20 and can be related to soil physical and chemical properties (Panagos et al., 2014). Direct assessments of the soil erodibility are only available at a plot scale. Large scale erosion studies employ transfer functions that infer the soil erodibility from soil properties that are easier to acquire. Several global soil data products are available that provide physical and chemical soil properties with different spatial resolution. We implemented soil information from SoilGrids250m (Hengl et al., 2017) and the Global Soil Dataset for use in Earth System Models (GSDE, Shangguan et al., 2014). Layers of mass fractions of sand (Sa),
25 silt (Si), and clay (Cl), the soil organic carbon content (orgC) and the fraction of coarse fragments (CRF) were acquired for the available soil depths and weighted average values for 0-10 cm were calculated. The aggregated soil layers were used in three transfer functions that were employed in previous large scale studies to compute K. We applied the method of Wischmeier and Smith (1987) and followed the procedure suggested by Panagos et al. (2014) and Borrelli et al. (2017) to compute K from the SoilGrids250m layers. The method of Wischmeier and Smith (1987) requires Sa, Si, Cl and organic matter content (OM)
30 as inputs. Additionally, information on soil structure (s) and soil permeability (p) is relevant. Borrelli et al. (2017) derived these properties from soil classes according to the World Reference Base (WRB) and the USDA soil texture classification systems that are available for SoilGrids250m. GSDE does not provide soil class layers. Thus, the parameters s and p were kept constant when using the GSDE as input, following a procedure by Tamene and Le (2015). We further implemented the methods of Williams (1995) and Torri et al. (1997). Both methods require values of Sa, Si, Cl and OM as inputs. The soil

products SoilGrids250m and GSDE in combination with three transfer functions resulted in six realizations of the K factor (Fig. 2b)).

The slope length and steepness factor LS represents the influence of the terrain topography on soil erosion (Panagos et al., 2015b). A digital elevation model (DEM) is the basis to derive the LS factor. In this study we implemented the SRTM v4.1

5 90m DEM (Jarvis et al., 2008) and the ASTER GDEM V2 (NASA/METI/AIST/Japan Spacesystems, and U.S./Japan ASTER Science Team, 2009) with a 30m resolution. ASTER GDEM V2 data was aggregated and projected to the 90m grid of SRTM v4.1 for comparability, but also because our computation capacities were insufficient to calculate soil erosion rates on a 30m grid for the study extent. Three methods were applied from Moore et al. (1991), Desmet and Govers (1996), and Böhner and Selige (2006) that are available from the System for Automated Geoscientific Analyses (SAGA) v. 2.1.4 (Conrad et al., 2015).

10 Together with the two DEM products six realizations of the LS factor (Fig. 2c)) were computed. Intermediate steps such as the reprojection of the ASTER GDEM V2, DEM fill, the calculation of flow direction or flow accumulation were processed in ArcMap 10.6 (ESRI, 2012). In the calculation of LS using the method of Desmet and Govers (1996) we followed the steps described in Panagos et al. (2015b). The use of ASTER GDEM v2 introduced strong noise in the computed LS layers that results from artifacts in the remote sensing data. Particularly, the computed soil erosion in flat areas was strongly affected by

15 the noise signal, rendering the result unusable. Thus, we excluded the LS realizations using ASTER GDEM v2 in the analysis and only considered three out of the six generated realizations for the LS factor (Fig. 2 c)).

The cover management factor C subsumes the impacts of vegetation cover and land management on soil erosion (Wischmeier and Smith, 1987; Panagos et al., 2015c). For large scale studies we identified two main approaches to compute C (Fig. 2d)); i) to infer C from vegetation indices from satellite based remote sensing products (e.g., Karamage et al., 2017; Naipal

20 et al., 2015; Tamene and Le, 2015; Van der Knijff et al., 2000) and ii) to join land cover classification products with agricultural statistics and C factor literature values to compile a continuous C factor layer (e.g., Borrelli et al., 2017; Panagos et al., 2015c; Bosco et al., 2015; Yang et al., 2003).

For the computation of C from NDVI vegetation indices we implemented the method of Van der Knijff et al. (2000), who proposed a non linear relationship between NDVI and C. We acquired 16 day MODIS NDVI averages (Didan, 2015) from

25 2000 to 2012 and aggregated them to a mean NDVI layer. We calculated the annual mean NDVI (see e.g., Van der Knijff et al., 2000; Tamene and Le, 2015) and the mean NDVI averages over the two rainy seasons March to May and October to November as proposed by Karamage et al. (2017). Both long-term mean NDVI layers were used to compute C factor realizations with the equation of Van der Knijff et al. (2000).

Two land cover products, the MODIS Collection 5 LC with a spatial resolution of 250m (Channan et al., 2014; Friedl et al.,

30 2010) and the ESA CCI LC Map v2.0.7 with a spatial resolution of 300m (ESA, 2017) served as base layers for the join with agricultural statistics and C factor literature values. Two agricultural statistics were used that provide information on crop areas at different spatial scales. i) National agricultural surveys for Kenya on ward level (KNBS, 2015) and for Uganda on county level (UBOS, 2010) were harmonized. ii) Monfreda et al. (2008) provides global gridded crop shares of 175 crops with a spatial resolution of 5 minutes. We assigned C factor literature values from Panagos et al. (2015c) and Angima et al.

35 (2003) to all crops found in the national agricultural surveys and the grid layers from Monfreda et al. (2008). Based on the

crop shares in the administrative units of Kenya and Uganda and for the crop shares in each grid cell of Monfreda et al. (2008) we calculated weighted average C values as proposed in Panagos et al. (2015c). C values for non agricultural land uses of the MODIS LC were estimated according to Panagos et al. (2015c) varying the C values for forest between boundaries based on the MODIS vegetation continuous fields (VCF) tree cover product. ESA CCI LC classifies the land cover as shares between

5   different land uses (e.g. Mosaic cropland (>50%) / natural vegetation (tree, shrub, herbaceous cover) (<50%)). In this case, C values were estimated by calculating weighted averages between the calculated average C values for agricultural areas and literature values (Panagos et al., 2015c) for non agricultural land uses according to the given fractions of the land cover classes. The combination of the two land cover products and the two agricultural statistic products resulted in four realizations for the C factor.

10 **3.3   Estimation of soil loss**

In total 7, 6, 6 (3), and 6 realizations were generated for the USLE input factors R, K, LS, and C, respectively. The combination of all input factors to assemble USLE model setups resulted in 1512 realizations of the USLE model. The LS factor realizations that were generated with the ASTER GDEM V2 were however excluded from the model ensemble, as they showed large noise ratios and the number of analyzed USLE model setups was therefore halved to 756. For the overlay of the generated USLE

15 input layers, all layers were reprojected to the grid of the SRTM v4.1 90m DEM and the long-term mean annual soil loss A was calculated for all model combinations in the study region of Kenya and Uganda using Eq. 1.

3.4   Analysis of spatially distributed soil loss estimates

The ensemble of 756 spatially distributed soil loss estimates with spatial resolution of 90 m were summarized in each grid cell employing descriptive statistical measures. In each grid cell we calculated mean and median values to estimate an average soil

20 loss from the USLE model ensemble. The range of the minimum and maximum soil loss A in a grid cell indicates the variation of the ensemble simulations in a grid cell (i.e. the disagreement between the model setups).

A common concept in the erosion literature is to relate soil loss to soil formation rates and therefore classify the soil loss as sustainable (tolerable) or non-sustainable (e.g., Blanco-Canqui and Lal, 2008; Montgomery, 2007; Van-Camp et al., 2004), or to group soil loss based on the severity of soil removal (e.g., Zachar, 1982; FAO-PNUMA-UNESCO, 1980). Suggested

25 tolerable levels of soil loss (T) vary between 5 and 12 $\mathrm{tons\ ha^{-1}\ yr^{-1}}$ on a global scale (Montgomery, 2007; Blanco-Canqui and Lal, 2008; Zachar, 1982). Karamage et al. (2017), Bamutaze (2015), Morgan (2009), or Lufafa et al. (2003) used 10 $\mathrm{tons\ ha^{-1}\ yr^{-1}}$ as threshold value T for studies conducted in Eastern Africa. For soil loss levels larger than T we implemented the soil loss classification after FAO-PNUMA-UNESCO (1980, implemented e.g. in Hernando and Romana (2015) or Olivares et al. (2016)) where a soil loss between 10 and 50 $\mathrm{tons\ ha^{-1}\ yr^{-1}}$ is considered to be moderate, a soil loss between 50 and

30 200 $\mathrm{tons\ ha^{-1}\ yr^{-1}}$ to be high, and a soil loss larger than 200 $\mathrm{tons\ ha^{-1}\ yr^{-1}}$ to be severe. In each grid cell we classified the simulated soil losses from the 756 USLE model setups into the four defined soil loss classes and calculated the frequencies for each soil loss class as follows:
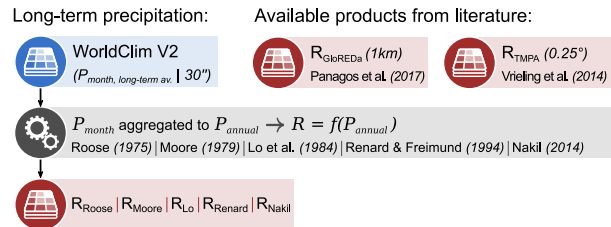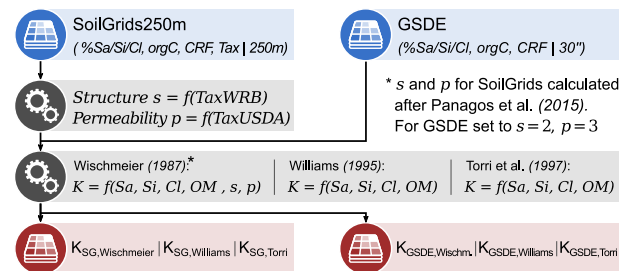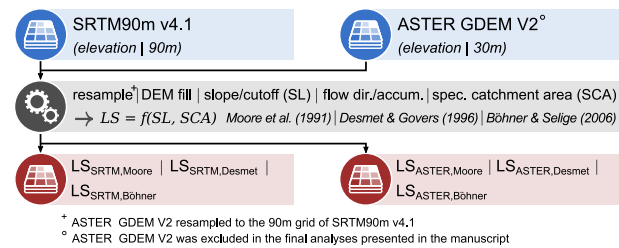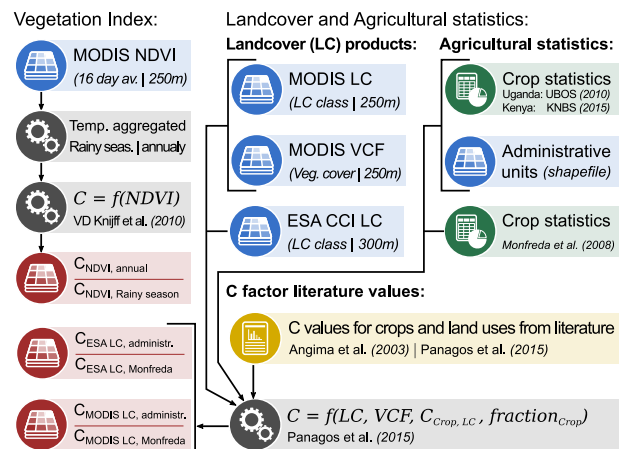
Figure 2. Methodological framework to generate the realizations of the USLE model input factors R, K, LS, and C.

$$f_{i,m,n} = \begin{cases} 0 & \text{if } A_{i,m,n} \notin [A_{class,lower}; A_{class,upper}) \\ 1 & \text{if } A_{i,m,n} \in [A_{class,lower}; A_{class,upper}) \end{cases} \tag{2}$$

$$f_{m,n} = \frac{\sum\limits_{i=1}^{N} f_{i,m,n}}{N} \tag{3}$$

where $f_{m,n}$ is the frequency of models that calculated a soil loss between the defined boundaries $A_{class,lower}$ and $A_{class,upper}$ of the respective class in the grid cell (m,n) and based on the $N = 756$ USLE model setups. A step function assigns the proba-

5 bilities $p_{i,m,n} = 1$ or $p_{i,m,n} = 0$ to a model i if the soil loss $A_{i,m,n}$ that was calculated with the model i for the grid cell (m,n) is included or excluded from a class interval.

3.5 Analysis of the USLE input factors

In the case of a simple model, such as the USLE, uncertainties in the inputs can be analytically propagated through the model to infer the uncertainties in the outputs (Beven and Brazier, 2011). Thus, the sensitivity of the calculated soil loss for the ranges

10 of the input factors can be analyzed analytically. We assessed the importance of the USLE input factors on the simulation of the soil loss in each grid cell by calculating the fraction between the range in soil loss that is caused by an input factor I_j and the total range of A that results from the entire model ensemble in that grid cell:

$$s_{j,m,n} = \frac{(\max(I_{j,m,n}) - \min(I_{j,m,n})) \cdot \prod\limits_{k \neq j} \max(I_{k,m,n})}{\left(\prod\limits_{k} \max(I_{k,m,n}) - \prod\limits_{k} \min(I_{k,m,n}) \right)} \tag{4}$$

where $s_{j,m,n}$ is the sensitivity of the input factor I_j in the grid cell (m,n), I is the set of the analyzed input factors R, K,

15 LS, and C, and k is the index of the respective input factor. The resulting sensitivity measure is normalized between 0 and 1, where a sensitivity $s_{j,m,n} = 1$ means that the total range of the calculated soil loss can result from varying the input I_j and 0 means that this input shows no variation between its realizations in the grid cell (m,n). In each grid cell the input factors are ranked based on their sensitivities and visualized to get a spatial reference of the importance of the model inputs.

3.6 Analysis of soil loss on administrative level

20 We assessed the soil loss on administrative levels for 27 administrative units in Uganda and Kenya. For all administrative units and all USLE model setups the mean soil loss was calculated. The distribution of the mean soil loss in each administrative units was analyzed with descriptive statistics. Employing Eq. (3) soil loss levels were determined for all grid cells in the respective administrative units and for all USLE model setups. The areas of each soil loss class calculated from all USLE model setups per administrative unit were summed up to compute the average share of a soil loss class for each administrative unit. Only

administrative units located in the erosion prone regions that are indicated in Fig. 1 are analyzed in the main document below. A complete summary of the results for all counties of Kenya and districts of Uganda can be found in the supplementary document in section S.3.

3.7 Comparison of the soil loss estimates to in field assessments

To provide a reference for the USLE ensemble simulations we used literature values of long-term mean annual soil loss from in-field assessments. García-Ruiz et al. (2015) compiled a comprehensive literature review for global soil loss rates, where three sources provided values for five sites within the study area of Kenya and Uganda. All three sources, however, applied different methods to assess the soil loss and cover a wide range of spatial domains. Sutherland and Bryan (1990) estimated the soil loss from the 0.3 km^2 Katiorin catchment located in the Lake Baringo drainage area in Kenya based on an in-stream discharge and suspended sediment sampling. Sutherland and Bryan (1990) estimated an average soil loss for the Katiorin catchment of 73 tons ha^{-1} yr^{-1} with a range between 16 and 96 tons ha^{-1} yr^{-1}. Kithiia (1997) reported results from soil loss monitorings in tributaries of the Athi River Basin conducted by the Kenian Ministry of Water Development. From the tributary sampling sites in the Athi River Basin we selected the 41 km^2 Riara catchment with an average reported sediment load of 1474 tons yr^{-1} (0.36 tons ha^{-1} yr^{-1}). Bamutaze (2010) preformed an erosion plot experiment in the Sinje catchment at Mt. Elgon in Uganda. Based on a two year monitoring, Bamutaze (2010) estimated a mean soil loss of 0.838 tons ha^{-1} yr^{-1} with a range between 0.185 and 1.761 tons ha^{-1} yr^{-1}. De Meyer et al. (2011) assessed the soil loss from 36 farm compounds in the two villages Iguluibi and Waibale close to the northern shore of Lake Victoria in Uganda. De Meyer et al. (2011) assessed the soil loss by reconstructing the historic surface level and calculating the lost soil volume. The estimations range between 56 and 460 tons ha^{-1} yr^{-1} in Iguluibi and 27 and 135 tons ha^{-1} yr^{-1} in Waibale.

To compare the ensemble soil loss estimations in this study with the literature values we calculated mean soil losses for grid cells that cover the original study site locations. Statistical measures were aggregated for the calculated site averages and plotted against the measured soil losses acquired from the selected studies.

3.8 Used software

The entire calculation of the USLE model realizations, most part of the input factor generation and the entire analysis of the simulation results was performed in the R programming environment (R Core Team, 2019). Spatial tasks and analyses were performed using the spatial R packages `raster` (Hijmans, 2019), `sf` (Pebesma, 2018), `rgdal` (Bivand et al., 2019), and `fasterize` (Ross, 2018). Data handling with SQLite data bases was managed through interfacing with the `RSQLite` (Müller et al., 2018) and `dbplyr` (Wickham and Ruiz, 2019) packages. Data analyses employed the R packages `dplyr` (Wickham et al., 2019b), `forcats` (Wickham, 2019), `lubridate` (Grolemund and Wickham, 2011), `purrr` (Henry and Wickham, 2019), `tibble` (Müller and Wickham, 2019), and `tidyr` (Wickham and Henry, 2019). Parallel computing to run some analyses was performed with the R packages `foreach` (Microsoft Corporation and Weston, 2017b), `doSNOW` (Microsoft Corporation and Weston, 2017a), and `parallel` (R Core Team, 2019). LS factor realizations were generated with the LS

Module in SAGA GIS (Conrad et al., 2015). Spatial maps were prepared in ArcGIS (ESRI, 2012) and in the R environment `ggplot2` (Wickham et al., 2019a) was used for all other figures.

4 Results

4.1 Analysis of the soil loss simulated with the USLE model ensemble

5 Overall, the calculated soil losses by our models follow the spatial pattern indicated by the potential erosion risk from topography that was presented in Fig. 1a). Both, the ensemble mean (Fig. 3a)) and the median soil loss (Fig. 3b)) show increased soil losses where moderate or high erosion risks were identified based on the slope thresholds suggested by Ebisemiju (1988). Mean soil losses of larger than 50 $\text{tons ha}^{-1} \text{ yr}^{-1}$ were found in the south-western corner of Uganda around Lake Bunyoni and along the Rift Valley in the North-West of Kenya. Particularly, excessive soil losses that exceed 200 $\text{tons ha}^{-1} \text{ yr}^{-1}$ were

10 calculated for the steep slopes around the Ruwenzori Mountains, Mt. Elgon, and Mt. Kenya with ensemble mean soil losses of up to 1865, 1663, and 1438 $\text{tons ha}^{-1} \text{ yr}^{-1}$, respectively. Large variations in the calculated soil losses in each grid cell in combination with highly positively skewed distributions are two reasons why the calculated mean soil losses are generally larger than the median values.

The strong discrepancy between the USLE model setups is evident from the comparison of the minimum calculated soil
15 losses (Fig. 3c)) and the maximum soil losses (Fig. 3d)) in each grid cell. While combinations of USLE model input factors were present in the model ensemble that calculated soil losses below 10 $\text{tons ha}^{-1} \text{ yr}^{-1}$ for 99 % of the study region and soil losses below 100 $\text{tons ha}^{-1} \text{ yr}^{-1}$ for the entire study region, other input factor combinations resulted in soil losses above 200 $\text{tons ha}^{-1} \text{ yr}^{-1}$ for over 45 % of the study region and substantial soil losses of at least 50 $\text{tons ha}^{-1} \text{ yr}^{-1}$ for over 85 % of the study region.

20 Fig. 4 provides a different perspective of the same ensemble simulations. Each grid cell shows the frequency for the defined soil loss levels *tolerable*, *moderate*, *high*, and *severe* (panels a)-d) respectively) that were predicted by the model members of the ULSE model ensemble. For large areas in the Northern Region of Uganda, the south of the lakes Kyoga and Albert in Uganda, and the Northeast Province and the northern parts of the Eastern Province in Kenya over 90 % (and in many cases all) of the USLE model setups calculated tolerable soil losses. In the topographically heterogeneous regions of the Uganda Plateau,
25 the South West of Uganda and the Gregory Rift in Kenya, a substantial share of up to 40 % of all model setups calculated a tolerable soil and the majority of model setups resulted in moderate soil losses. Only along the steep mountain ridges in the Rift Valley and the mountain massifs of Mt. Kenya, Mt. Elgon, the Ruwenzori Mountains and the region around Lake Bunyoni a substantial part of USLE model setups calculated high and severe soil losses (yellow and local red regions in Fig 4 c) and d)).

Fig. 5 combines the soil loss classification and the (un)certainties in the prediction of soil loss levels based on the USLE
30 model ensemble into one representation. The dominant soil loss levels that a majority of model setups predicted for a grid cell are shown in green (*tolerable*), blue (*moderate*), orange (*high*), and purple (*severe*). The lightness of the colors indicates the percentage of models that calculated a soil loss within the respective soil loss classes. To highlight the complex patterns that
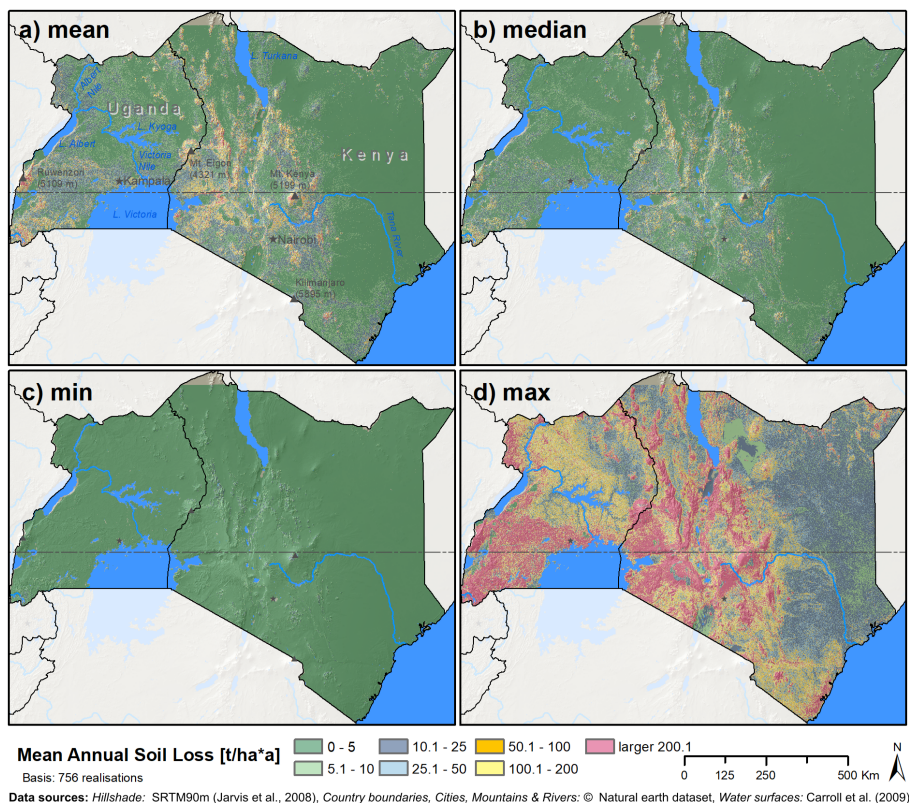
Figure 3. Descriptive statistics calculated for each grid cell based on the 756 USLE model realizations. Panels a) to d) show the mean, median, minimum, and maximum long-term annual soil erosion in each grid cell.

result from the ensemble soil loss estimations in topographically heterogeneous regions, we show the Mt. Elgon (Fig. 5 b)), Lake Bunyoni (Fig. 5 c)), and Mt. Kenya (Fig. 5 d)) regions in detail.

The strong agreement between the USLE model setups to calculate tolerable soil loss for the generally flat regions of Kenya and Uganda (shown in purple in Fig. 4 a)) is visible in dark green in Fig. 5 a). The soil loss level patterns in the erosion prone

5 areas of Mt. Elgon, Lake Bunyoni, and Mt. Kenya clearly follow the topographic patterns of these regions, with high and severe soil loss levels along the mountain ridges and tolerable to moderate soil losses in the valley bottoms. The agreement of the USLE model setups to predict the same soil loss level in such heterogeneous topographies is generally lower, showing percentages of 25 to 75 %. Only along the very steep slopes of the mountain massifs (and particularly at the top of Mt. Kenya with its steep slopes and low vegetation cover) a large majority of the USLE model ensemble predicted a severe soil loss (center

10 of Fig. 5 d)). Although the entire Mt. Elgon and the Mt. Kenya massifs show moderate to steep slopes (see. Fig. 1 b)), a large majority of the USLE model ensemble (>75 %) calculated tolerable soil losses for the densely forested northern part of Mt. Elgon and the forest belt around Mt. Kenya.
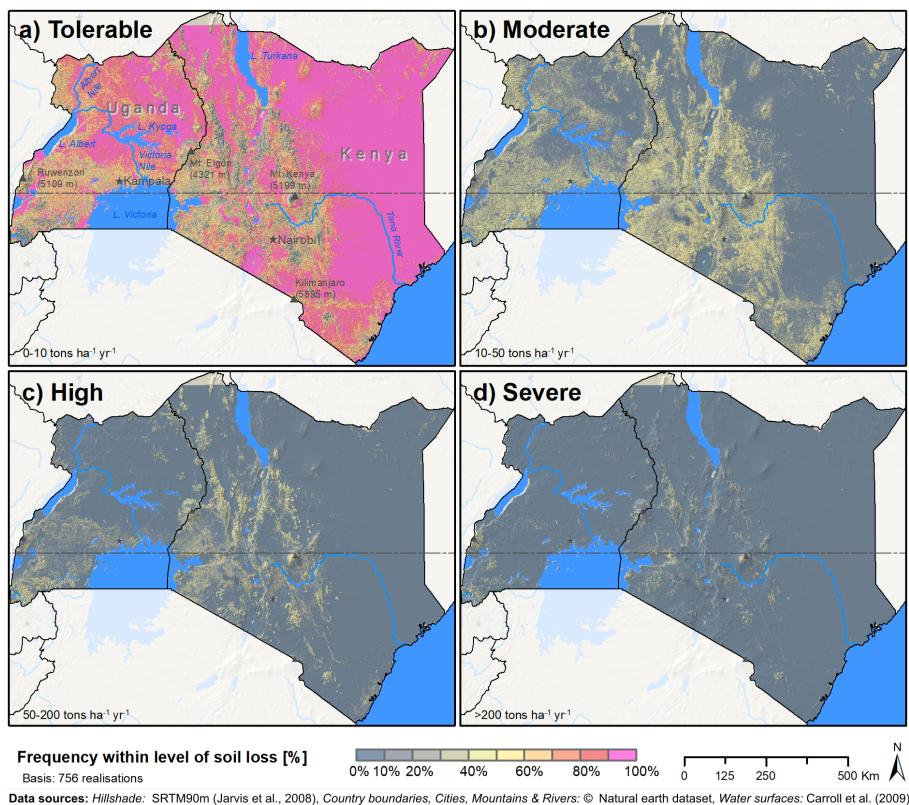
Figure 4. Frequency of USLE model ensemble members to predict one of the four soil loss classes *tolerable* $(0 - 10 \text{ tons ha}^{-1} \text{ yr}^{-1})$ (a), *moderate* $(10 - 50 \text{ tons ha}^{-1} \text{ yr}^{-1})$ (b), *high* $(50 - 200 \text{ tons ha}^{-1} \text{ yr}^{-1})$ (c), and *severe* $(>200 \text{ tons ha}^{-1} \text{ yr}^{-1})$ (d), based on the soil loss classification after FAO-PNUMA-UNESCO (1980). The pixel color illustrates the percentage of models from the model ensemble that calculated a soil loss in between the respective class boundaries.

4.2 Analysis of the USLE input factors

The range of the calculated soil loss A in a grid cell is the direct result of the different values stemming from the various input factor realizations. A large range in the values of an input factor in a grid cell has a greater impact on the resulting uncertainties of the calculated soil loss compared to input factors where the different realizations show similar values. The analysis of the

5   strongest impact of input factors on the uncertainties of A revealed clear spatial patterns at different spatial scales (Fig. 6 a)). Over the whole domain, the input factors C, K, and LS were identified as the most important inputs for the uncertainties in soil loss in 34.74%, 31.39%, and 28.55% of the total study area, respectively. The R factor was only locally identified as the most relevant input factor in 5.32 % of the total study area. The C factor and the K factors show large aggregated patterns in both countries. The importance of the LS factor, however, generally shows small structured, heterogeneous patterns scattered

10   over the entire study region. Exceptions are visible in larger depressions along the Gregory Rift in zones where the slope is close to 0. Lake Magadi (100 km^2), an alkine lake located in an endorheic basin in the Rift Valley south of Nairobi, or a larger
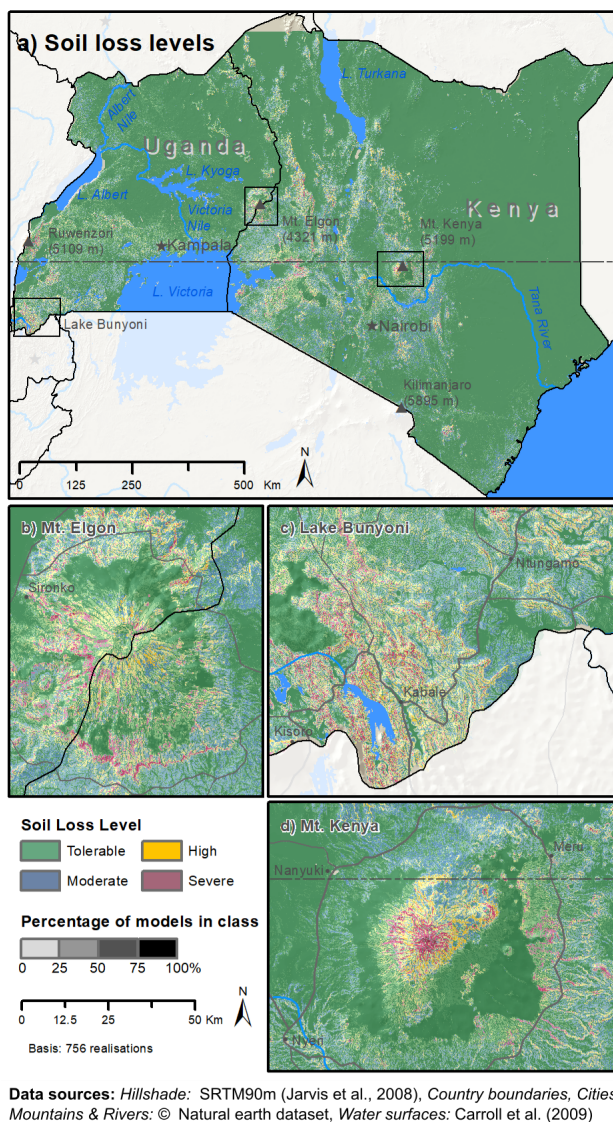
Figure 5. Dominant soil loss levels. The color shows the soil loss level predicted by the majority of USLE model setups. The lightness of the color indicates the percentage of models that predicted the dominant soil loss level. Panel a) shows the study area of Kenya and Uganda. The panels b), c), and d) show erosion prone areas around Mt. Elgon, Lake Bunyoni, and Mt. Kenya, respectively.

region in the east of Lake Turkana are the most distinct examples for large patterns of LS. Clusters of high importance of the R factor were only identified in high altitudes with generally large precipitation sums, but also in very dry regions in the northern Kenya, where the precipitation sums are close to 0.

Fig. 6 b)-d) provides more detail of the spatial patterns of the input factors and their importance for the calculation of the
5   soil loss in regions around Mt. Elgon, Lake Bunyoni, and Mt. Kenya (that were also analyzed in Fig 5). In contrast to Fig. 6
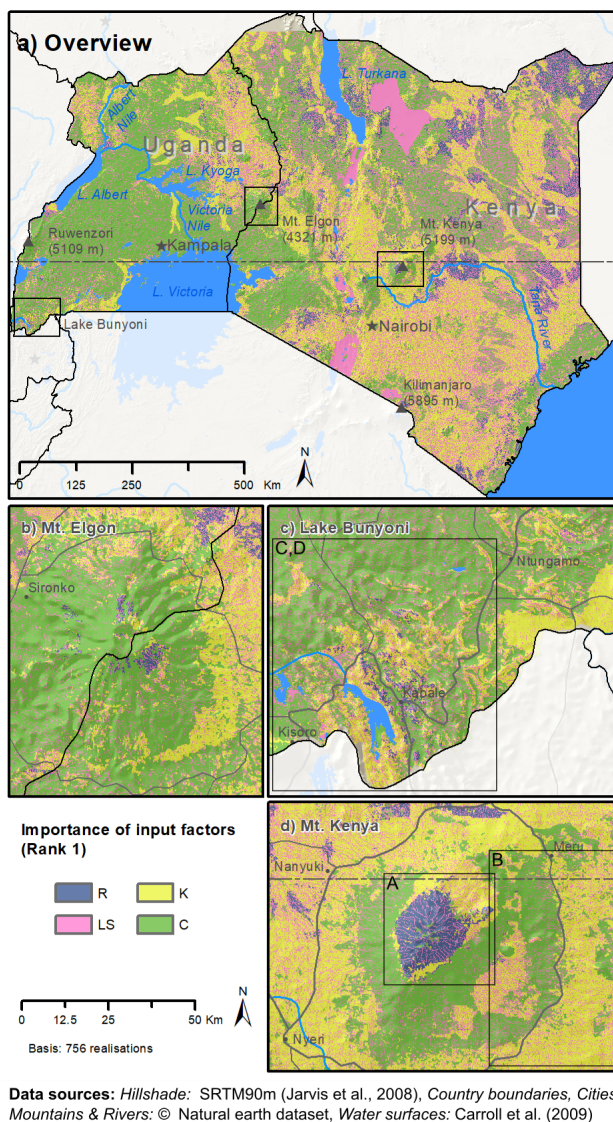
Figure 6. Most important USLE model input factors for the calculation of the soil loss A. The colours blue, yellow, pink, and green indicate whether the input factors R, K, LS, or C caused the largest range in the calculation of A in a grid cell. Panel a) shows the study area of Kenya and Uganda. The panels b), c), and d) show critical erosion hot spots around Mt. Elgon, Lake Bunyoni, and Mt. Kenya, respectively. The insets A) to D) indicate the extents for which the input factor realizations for R, K, LS, and C were analyzed in Fig. 7.

a), finer-scale characteristics of input factor importance become visible. The patterns around the two mountains Mt. Elgon and Mt. Kenya show similarities. Although the R factor is spatially highly concentrated at the top of Mt. Kenya and only slightly visible on the east of Mt. Elgon, both regions show a high importance of the R factor for the calculation of A in high altitudes. High altitude areas are mostly characterised by a sparse observation network for precipitation. R is highly correlated to some,

in our case spatially distributed, rainfall estimates. High uncertainties in rainfall records, but also in the modelling chain to derive remotely sensed precipitation explain these patterns. Moving down from the summits, belts of a high importance of the C and K factor are visible. These distinct patterns result from the vertical bands of changes in vegetation in such mountainous regions and the impact of sparse and dense natural vegetation and agricultural land uses on the calculation of the C factor. The

5   Lake Bunyoni region shows more heterogeneous patterns for the most important input factors. In the north, the calculation of A is affected by the C factor in large regions and the LS factor on very small scaled patterns. In the east and west of Lake Bunyoni, patterns for all input factors are visible that follow the terrain topography. The LS and K factor are the most relevant input factors for the calculation of A along the ridge lines, while the C factor becomes more important closer to the valley bottoms.

10   The importance of an input factor for the calculation of A results from the differences in the estimated input factor values for the individual input factor realizations. In Fig. 7 we analyzed the input factor realizations of R, K, LS, and K in the four regions A) to D) (indicated in Fig. 6). For the analysis only grid cells in the defined extents A) to D) were selected, which had the condition (i) that the respective input factor was the most relevant one and (ii) where the soil loss was calculated to be high to severe.

15   Case A) (Fig. 7 A)) shows the differences of R at the top of Mt. Kenya. Generally, a difference between the rainfall erosivity products derived from temporally high resolution rainfall (GloREDa (Panagos et al., 2017) and TMPA (Vrieling et al., 2014)) and the distributions of the R values obtained from long-term annual precipitation is visible. While both, GloREDa and TMPA show low R values between 1869 and 3486 MJ mm ha^{-1} h^{-1} yr^{-1} and 3000 and 4602 MJ mm ha^{-1} h^{-1} yr^{-1}, respectively, the methods of Roose (1975), Moore (1979), Renard and Freimund (1994), and Lo et al. (1985) resulted in a wide range of R

20   values between 4940 MJ mm ha^{-1} h^{-1} yr^{-1} (minimum value using the method of Lo et al. (1985)) and 16207 MJ mm ha^{-1} h^{-1} yr^{-1} (maximum value using the method of Roose (1975)). Hence, a strong impact of the selected equation to calculate R from long-term annual precipitation is observable. Only the method of Nakil (2014) showed low R values in the same range as GloREDa and TMPA, with a range between 2590 and 3757 MJ mm ha^{-1} h^{-1} yr^{-1}. The method of Nakil (2014), however, generally generated very low R values (also where GloREDa and TMPA showed significantly larger R values).

25   Case B) (Fig. 7 B)) compares the K factor realizations in the south-eastern belt around Mt. Kenya. The six realizations of K show a clear pattern that is strongly affected by the methods that were employed to calculate K, while the differences between the two soil products that were used are rather insignificant. The method of Torri et al. (1997) resulted in by far the largest K values between 0.069 tons h MJ^{-1} mm^{-1} and 0.088 tons h MJ^{-1} mm^{-1}. On average these values are three times larger than the ones calculated with the method of Williams (1995) (with a range between 0.021 tons h MJ^{-1} mm^{-1} and 0.031 tons

30   h MJ^{-1} mm^{-1}) and up to 13 times larger than the values calculated with the method of Wischmeier and Smith (1987) when using the SoilGrids data set (with a range between 0.011 tons h MJ^{-1} mm^{-1} and 0.028 tons h MJ^{-1} mm^{-1}).

Case C) (Fig. 7 C)) shows the differences between the the LS factor realizations along the ridges of the hills around Lake Bunyoni. Eventually only the SRTM 90m DEM was used as input data. Thus, Fig. 7 C) compares the three methods of Moore et al. (1991), Desmet and Govers (1996), and Böhner and Selige (2006). While the methods of Moore et al. (1991) and Böhner

and Selige (2006) resulted in comparable values with ranges between 1.47 and 3.90 and between 1.65 and 5.03, respectively, the method of Desmet and Govers (1996) resulted in five times larger values with a range between 8.22 and 18.79.

Case D) (Fig. 7 D)) compares the implemented C factor realizations for the same extent around Lake Bunyoni as it was used in case C). In general two patterns are observable. A strong difference between the realizations that employ the NDVI as input and the C factor realization that were derived from land cover products and literature C factor values is visible. Further, using the gridded crop distribution product of Monfreda et al. (2008) to derive spatially distributed mean C factor values from the literature resulted in larger values compared to the implementation of agricultural census data on the administrative unit level for Kenya and Uganda. The impact of the used land cover product (ESA LC or MODIS LC) are low. Both realizations based on NDVI (NDVI, annual and NDVI, rainy season) show mean C factor values of 0.04 and 0.03, respectively. The C values for the realizations that employed crop data from Monfreda et al. (2008) and agricultural census data were on average six times and 4.5 times larger with mean values of 0.21 and 0.15 respectively.

4.3 Soil loss at the administrative level

The selected administrative units in Uganda and Kenya are located in erosion prone areas (shown in Fig. 3 and Fig. 4). Averaging the soil loss for the domain of an administrative unit reduces the impact of areas with excessive soil loss. Nevertheless, the median values of mean soil loss for the selected administrative units that result from the USLE model ensemble result in a moderate (blue) soil loss in 22 of the 27 administrative units. Four administrative units show even a high (yellow) mean soil loss, while only one administrative unit resulted in a tolerable (green) soil loss (Fig. 8 a)). Particularly large mean soil losses were found for the administrative units Kabale and Kisoro in the Lake Bunyoni region and the administrative units Kasese and Bududa on the slopes of the Ruwenzori Mountains and Mt. Elgon, respectively. The data points shown as coloured squares in Fig. 8 a) provide a reference to the soil loss assessment performed by Karamage et al. (2017) on district level in Uganda. As we included the realizations of the USLE input factors developed in Karamage et al. (2017) in the present assessment, the calculated soil loss from Karamage et al. (2017) is a member of the USLE model ensemble. In 9 of the 16 districts the soil losses calculated by Karamage et al. (2017) are lower than the 25 % quantile of soil losses that resulted from the USLE model ensemble. Only for a few districts, such as Kasese, Bundibugyo, Nebbi, or Kaabong the soil losses calculated by Karamage et al. (2017) and the ensemble means show comparable values.

For each administrative unit, the mean soil losses that resulted from the individual USLE model ensemble members show wide spreads (indicated by box plots and light grey dots in Fig. 8 a)). The spreads were particularly large in the administrative units with overall high soil losses. In all administrative units the mean soil loss that resulted from the individual USLE model setups are scattered over several soil loss classes (class boundaries indicated by dashed lines in Fig. 8 a)). Fig. 8 b) summarizes the numbers of model setups that predicted one of the four soil loss classes for each administrative unit. Although the median soil loss class for the majority of the administrative units is *moderate* on average 49 % (370 out of 756 models; with a range of 25.4 % to 60.4 % between the 27 administrative units) of the models from the USLE model ensemble predicted moderate soil loss, while all other model setups predicted one of the other four soil loss classes.
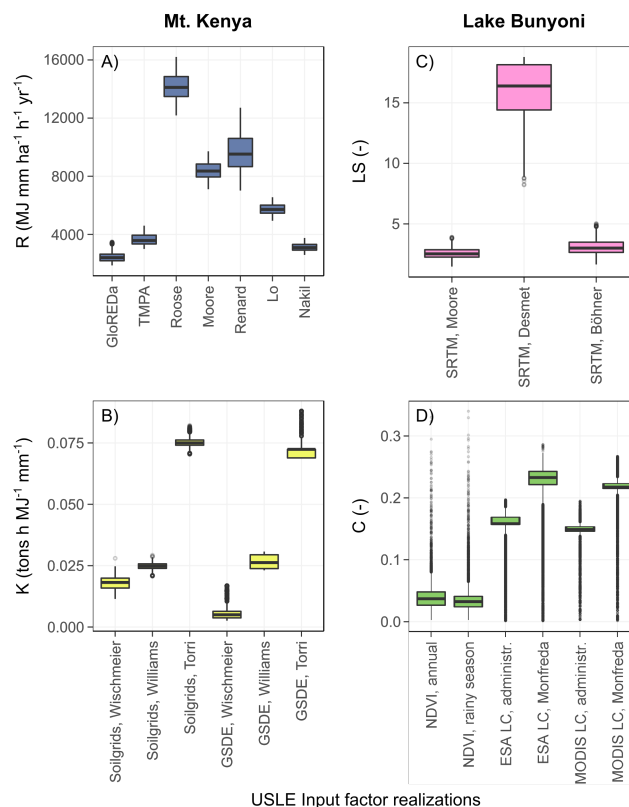
Figure 7. Variability between the realizations of the most important USLE model input factors. The cases A) to D) (delineated in Fig 6) exemplify the differences in the distributions of the input factor R, K, LS, and C, respectively. The cases A) to D) include the values of input factor realizations for grid cells, in which the respective input factor was the most sensitive one and high to severe soil loss was predicted to be likely. Panel A) analyzes the R factor realizations at the top of Mt. Kenya, panel B) shows the differences in the K factor realizations in the belt around Mt. Kenya, and the panels C) and D) analyze the LS and C factors in the hilly topography of the Lake Bunyoni region.

Fig. 8 c) relates the soil loss classification in the selected administrative units to the average shares of the soil loss classes in the administrative unit areas. While on average only 20 % of the models from the USLE model ensemble predicted a tolerable soil loss in the administrative units almost 55 % of the areas of the administrative units show on average a tolerable soil loss. Areas with high and severe soil loss share only small areas in the administrative units with average fractions of 14.5 % and 6.5 % respectively. Though, these areas have a strong impact on the mean soil loss in an administrative unit.

4.4 Comparison of the soil loss estimates to in field assessments

While the total ranges of the soil loss estimates calculated for the reference sites from the USLE model ensemble cover the reference soil losses from literature values in all five cases in Fig. 9 the interquartile ranges for the USLE model ensemble can strongly differ from the values that were estimated from in field experiments.
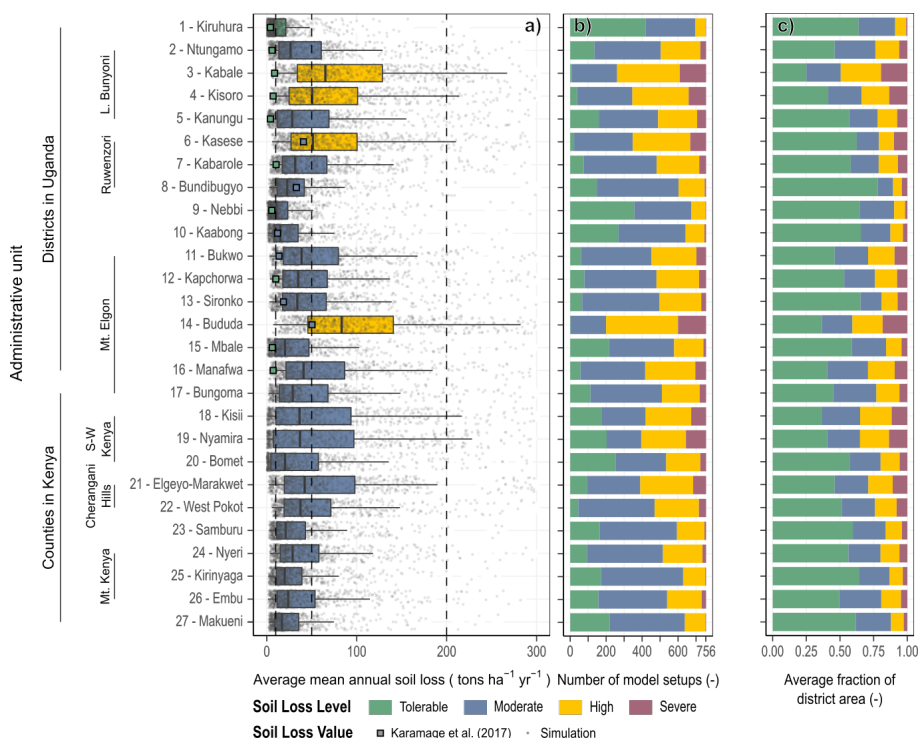
Figure 8. Mean soil loss in selected erosion prone administrative units of Uganda and Kenya. Panel a) shows the mean soil loss from all 756 USLE realizations in the selected administrative units with grey dots and aggregated as boxplots. The colors indicate whether the median soil loss in an administrative unit is *tolerable* (green), *moderate* (blue), *high* (yellow), or *severe* (purple). For comparison the results from Karamage et al. (2017) are plotted as colored squares. Panel b) shows the distributions of soil loss levels that were predicted by the USLE model realizations for the selected administrative units. Panel c) shows the average shares of soil loss classes for the domains of the selected administrative units.

Cases I and II in Fig. 9 compare average soil losses for the domains of the villages Iguluibi and Waibale to soil loss assessments of small scale farm compounds. In both cases the soil losses assessed in the field exceed the interquartile ranges that result from the USLE model ensemble, with ranges of 56 to 460 $\mathrm{tons\ ha^{-1}\ yr^{-1}}$ and 8.6 to 53.4 $\mathrm{tons\ ha^{-1}\ yr^{-1}}$ in Iguluibi and 27 to 135 $\mathrm{tons\ ha^{-1}\ yr^{-1}}$ and 3.1 to 16.2 $\mathrm{tons\ ha^{-1}\ yr^{-1}}$ in Waibale.

5   For the Sinje test case (case III in Fig. 9) in the Manafwa district in Uganda Bamutaze (2010) resulted in very low soil losses between 0.185 and 1.761 $\mathrm{tons\ ha^{-1}\ yr^{-1}}$. Generally the districts along Mt. Elgon are known to be erosion prone. On average the USLE model ensemble predicted high soil loss for the location of the Sinje test catchment with a median soil loss 86.8 $\mathrm{tons\ ha^{-1}\ yr^{-1}}$ and an interquartile range between 3.9 and 212 $\mathrm{tons\ ha^{-1}\ yr^{-1}}$. Although the range of calculated soil losses is generally large, only 11 % of models from the USLE model ensemble predict soil losses that are in the range of the values

10   reported by Bamutaze (2010).
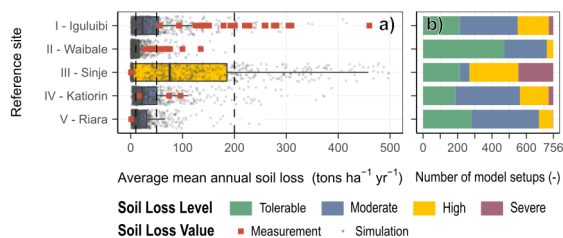
Figure 9. Comparison of soil loss simulations from the USLE model ensemble to in field soil loss assessments acquired from selected studies. The reference soil loss values are shown with red squares for the sites Iguluibi and Waibale (De Meyer et al., 2011), Sinje (Bamutaze, 2010), Katiorin (Sutherland and Bryan, 1990), and Riara (Kithiia, 1997) in panel a). The soil loss simulations for the reference extents from all 756 USLE model realizations are shown as grey circles. Corresponding boxplots show summary statistics for the model ensembles in panel a). Panel b) summarizes the numbers of models that predicted the soi loss levels *tolerable* (green), *moderate* (blue), *high* (orange), and *severe* (purple) for the reference sites.

The reported soil losses for the Katiorin catchment are comparable to the soil loss estimations for the catchments extent that resulted from the USLE model ensembles (case IV in Fig. 9). Sutherland and Bryan (1990) reports a range of soil loss between 16 and 96 $\mathrm{tons\ ha^{-1}\ yr^{-1}}$ for the Katiorin catchment and 21 % of the USLE model setups predict a soil loss in the same range. Almost 30 %, however, result in soil losses lower than 16 $\mathrm{tons\ ha^{-1}\ yr^{-1}}$.

5   Kithiia (1997) reports a very low soil loss of 0.36 $\mathrm{tons\ ha^{-1}\ yr^{-1}}$ for the Riara Basin. All USLE model realizations predict larger soil losses for the domain of Riara, with a minimum value of 1.6 $\mathrm{tons\ ha^{-1}\ yr^{-1}}$ and an interquartile range of 6.8 to 30.7 $\mathrm{tons\ ha^{-1}\ yr^{-1}}$.

5   Discussion

5.1   What can we learn from such an analysis

10   We illustrated how drastic the differences in the estimated soil loss magnitudes can be by selecting a method to calculate a USLE input factor. The statistical analysis of the generated USLE model ensemble (Fig. 3) showed that ranges of one or two magnitudes for the estimated soil loss were possible. These large ranges ultimately result from differences in the individual realizations of the USLE input factors (some realizations were over a magnitude larger than others in Fig. 7). These differences in the inputs propagate through the USLE equation by multiplication.

15   The immanent question that arises is whether we are able to exclude any combinations of USLE input factors or individual realizations of input factors, as they fail to result in plausible soil losses and eventually reduce the ranges in estimated soil losses (Beven, 2018; Beven and Brazier, 2011). From a modellers perspective, neither the comparison to observations (Fig. 9), nor a plausibility check of the individual USLE model realisations generally allowed us to exclude model combinations or individual methods for the generation of USLE inputs. As a consequence, we have to acknowledge the uncertainties that result

from commonly used methods to generate spatially distributed estimates of the USLE input factors and/or find additional ways to evaluate the simulated soil losses (see section 5.2).

In the case that model setups cannot be falsified and are considered as "fit-for-purpose" (Beven, 2018), we must treat each member of the ensemble equally. In Fig. 4 and Fig. 5, and Fig. 8 we proposed ways to utilize the generated USLE model
5 ensemble and infer the severity of soil loss on different spatial levels based on a compromise of many models. From a decision makers perspective, such large ranges in soil loss imply challenges in the interpretation of the results and complicate decisions on possible measures that can be implemented. Nevertheless, the analysis of soil loss on the administrative level (Fig. 8) and particularly the comparison to the results from Karamage et al. (2017) should highlight an example to favor the analysis of the entire possible uncertainty range in soil loss, as opposed to accepting a single prediction of soil loss as a basis for decision
10 making.

A possible approach to utilize the USLE ensemble predictions was presented in the combined assessment of soil loss levels that were predicted by the majority of the ensemble members and showed the fraction of models that predicted dominant soil loss levels in Fig. 4. Such reduction of information provided by the ensemble results enables to provide a "single" answer to the question of the severity of the soil loss to be expected and conveying the "certainty" of a prediction at the same time.
15 Though, thresholds that define a specific soil loss as tolerable, or critical are seen as controversial (Bosco et al., 2015) and a wide range thresholds for tolerable soil loss (e.g., Karamage et al., 2017; Bosco et al., 2015; Bamutaze, 2015; Blanco-Canqui and Lal, 2008; Montgomery, 2007) and soil loss classification schemes (e.g., Zachar, 1982; FAO-PNUMA-UNESCO, 1980) are proposed.

To illustrate the dominant soil loss level together with the frequency of models that predicted that soil loss level can strongly
20 support the evaluation of the model results. A large share of the USLE input factor combinations, for instance, predicted low soil losses along slopes with dense forest vegetation (see e.g. dark green area in Fig. 5 d)). Thus, reduced soil loss in densely vegetated areas can be expected with a higher certainty based on the ensemble predictions. In contrast, areas with sparse vegetation (e.g. close to the summit of Mt. Kenya in Fig. 5) show increased soil loss, but lower percentages of USLE model members that predict the respective soil loss level at the same time. These are potential zones where any form of validation or
25 plausibility check would benefit the analysis.

The analysis of the USLE input factor realizations with respect to their impact on the uncertainties of the simulated soil loss reveals patterns for the USLE inputs on different spatial scales in Fig. 6. These patterns can support in identifying the USLE inputs that require greater attention for the USLE model setup, based on the local conditions. Larger patterns were mainly visible for the input factors C and K, while LS showed very small scaled patterns and R showed a lower relevance for the
30 prediction uncertainties in general. While the C is clearly the most important input factor for large regions in the densely vegetated part of Uganda and around Lake Victoria in Kenya, K is most relevant in the drier regions of Kenya. The R factor was mainly relevant in higher altitudes. The LS factor realizations were most relevant in highly variable topographies and very flat areas where the factor is close to zero and numerical issues governed the results of the sensitivity analysis.

5.2   Are in-field data a valid reference for USLE model evaluation

No clear pattern can be defined from the comparison of estimated soil losses to in-field soil loss assessments within the study domain. The selected reference studies had different specific scopes. While Sutherland and Bryan (1990), or Kithiia (1997) monitored the accumulated soil loss from river catchments, De Meyer et al. (2011) assessed the soil loss on small scales and

5   on sites that are particularly erosion prone. While most of the selected reference studies report low to moderate soil losses for their study domains, De Meyer et al. (2011) reports high to excessive soil losses for several of the farm compounds they investigated. The methodologies that were used for the soil loss assessments strongly impacted the reported soil losses and result in wide ranges of soil loss between the selected studies.

Aforementioned limitations of the temporal and spatial representativeness of the reported soil losses from the selected

10   reference studies are likely to be present and may have impacted the significance of the comparison to the soil loss estimates. Boardman (2006) stresses that long-term monitoring schemes and additional assessments of rills and gullies would be required to allow a comparison to soil loss estimations. Records from erosion monitoring studies are, however, usually short (Evans, 2013; Govers, 2011). The reference studies of Sutherland and Bryan (1990) and Bamutaze (2010) for instance only covered monitoring periods of 1 and 2 years, respectively and thus are only snapshots in time that are difficult to compare with long-term

15   assessments.

Although the soil losses reported in De Meyer et al. (2011) are based on cumulative soil losses in farm compounds over periods of 15 to 20 years, the spatial domains of the farm compounds that were analyzed do not properly reflect the spatial resolution of the grid on which the soil loss assessment with the USLE was conducted. Other reference studies, such as Sutherland and Bryan (1990) or Kithiia (1997) better meet the spatial scale of the USLE soil loss assessment. However, the

20   presented soil yields are in-stream sediment loads. These reported loads are affected by processes, such as deposition, gully erosion, land sliding, or bank erosion that superimpose rill and inter-rill erosion (Govers, 2011). Boardman (2006) further highlights that the in-stream sediment delivery ratios (SDR) are a function of time and scale. Boardman (2006) compares the differences in the SDR of the Yellow River and British rivers that differ by a factor of 28. Such large difference in the SDR does, however, not necessarily reflect the differences in soil erosion rates.

25   Evans (1995) and Boardman (2006) point out that soil losses derived in plot scale experiments do not reflect erosion taking place on the landscape scale. Evans (1995) found that plot scale soil losses are larger than soil losses in the landscape by a factor of two to ten under comparable conditions. The soil losses reported in Bamutaze (2010) were however lower than the soil losses estimated by almost 90 % of all used USLE models in this study and thus show an opposite behavior.

Prasuhn et al. (2013), Warren et al. (2005), or Evans (2002), among others, demand that soil losses that were estimated by

30   models must be supported by field based observations. Bosco et al. (2015) emphasize the limitations of in-field validation for large scale studies. Bosco et al. (2014) and Bosco et al. (2015) highlight the potential to employ new high resolution satellite imagery and Google Earth, or Google Streetview data for plausibility checks of soil loss estimates. Yet, the verification (and falsification) of the absolute magnitudes of soil loss estimates on large scales remains a challenge.

5.3 Further considerations and limitations

In this study we only implemented a selection of methods and primary data sources for the calculation of the USLE input factors. Hence, we have to recognize that the performed study does not provide a comprehensive picture of the uncertainties that are introduced by different representations of the USLE input factors. Albeit, the calculated ranges in soil loss were substantial

5 and considering additional realizations of USLE input factors can in the worst case increase the ranges of calculated soil loss. The demonstrated procedure, however, pinpoints the central weakness of the USLE. The model can identify relative risks for soil erosion, but fails to predict exact magnitudes of soil loss. Eventually every modeller must acknowledge the limitations of the USLE (some of them we addressed at great length) and not overestimate the predictive power of the model.

We are fully aware that such a comprehensive analysis is very likely out of scope for most studies that employ the ULSE

10 model, as in most applications the soil loss estimation is only a small part of the entire analysis. Further, extending such analysis to larger domains or increasing the spatial resolution can be limited by available computation and storage capacities. For instance, the entire ensemble of USLE model representations in the present study comprised $11225 \times 14778 \times 1512$ (~$250 \cdot 10^9$) pixel values required 2.13 TB distributed in SQlite data bases on four separate hard drives to allow an efficient batch-wise analysis of the model results. Nevertheless, checking the plausibility of estimated soil loss must be the minimum requirement

15 for every study employing the USLE (see suggestion above and Bosco et al., 2015, 2014).

We omitted the analysis of the conservation support or management practice factor P in this study. For all USLE model setups the P factor was globally set to a value of 1. According to literature values, the application and maintenance of support practise measures can substantially reduce the soil erosion in erosion prone landscapes. Conservation measures, such as contour farming, strip cropping, or terracing reduces the calculated soil loss by a factor of up to 2, 4, and 10, respectively, depending

20 on the slope on which the measure was applied (Karamage et al., 2017). Large scale estimations of P and the implementation of the P factor in large scale soil loss assessments are almost absent, as only very limited spatial data is available on soil conservation measures. Panagos et al. (2015d) generated a spatial estimate for P for entire Europe, considering the effects of contouring, stone walls, and grass margins. Panagos et al. (2015d) thereby used comprehensive spatial statistics on soil conservation based on 270000 data points available for Europe from the LUCAS data base (LUCAS, 2012). Such detailed

25 data is, however, not available in all regions of the world. Thus, other large scale assessments omitted the P factor and used a value of 1 globally (e.g., Borrelli et al., 2017), assigned a reduced P value globally in the study domain (Karamage et al., 2017), or assigned global values for P to specific land uses (Yang et al., 2003). Such simplifications do not reflect the spatial distributions of soil conservation measures that are actually applied in a (large scale) study domain, although their impact on large soil loss estimates can be substantial.

30 ## 6 Conclusions

The USLE model, an empirical model to estimate the soil loss by water erosion is widely applied in large scale assessments and was implemented in a case study to assess the soil loss on the entire domain of Kenya and Uganda. Although the USLE has a simple model structure and is therefore easy to implement, the generation of spatially distributed estimates of the USLE input

factors for the study domain poses a major challenge. Large scale (remote sensing) data products and methods to employ them for the generation of the USLE inputs greatly support soil loss assessments on large scales. In order to analyze and quantify the impact of available data products and with methods for the calculation of USLE inputs on the uncertainties of estimated soil losses, we generated a range of realizations for each USLE input factor and combined them to 756 realizations of the USLE to
5 compute spatially distributed soil loss for entire Kenya and Uganda.

Overall, but particularly in erosion prone areas of the study domain, the calculated ranges of soil loss showed large values. In many cases, especially in areas with high soil losses, the calculated ranges exceeded the mean soil loss by greater than one order of magnitude. To condense the information provided by the USLE model ensemble we proposed to classify the soil loss into the soil levels *tolerable*, *moderate*, *high*, and *severe* employing common soil loss thresholds from literature. The classification
10 allowed to utilize the USLE ensemble predictions to analyze but consider the "certainty" of the prediction simultaneously. The employed approach enabled to identify zones with increased soil loss, but also areas where the agreement in the USLE model ensemble is low and thus suggest an evaluation and/or plausibility checks for the simulations.

A sensitivity analysis of the soil loss predictions was performed to identify the USLE input factors that introduce the strongest impact on the uncertainties of the soil loss estimates. The analysis identified clear patterns on the large scale for the input factors
15 C and K, where the C factor is more relevant for areas with denser vegetation and the K factor showed a greater importance for the calculation of the soil loss in dry less densely vegetated areas. The LS factor showed very scattered patterns in complex topographies and was relevant for the uncertainties of the calculated soil loss in sloped terrain.

A validation of simulated soil loss on large scale domains, employing in-field assessments from the literature poses to be a challenge and in this study no clear conclusions can be drawn for the ensemble soil loss estimates when they were compared to
20 soil loss observations. Thus, the comparison failed to falsify any of the generated USLE model combinations that would allow to exclude ensemble members to ultimately reduce the soil loss prediction uncertainties. Major issues for a valid comparison are the differing origins of the in-field soil loss data as well as spatial and temporal limitations of the observed data.

Although available computational and time resources will naturally limit such an analysis of soil loss predictions in most studies that employ the USLE model, the findings clearly highlight the importance to critically view and analyze single USLE
25 model predictions, as the resulting soil loss estimates are highly sensitive to the combinations of realizations of the USLE model inputs. We further question the aptitude of soil loss assessments based on in-stream sediment yields or small scale plot experiments to be valid data for the evaluation of soil loss estimates and want to refer to new approaches (e.g. Bosco et al., 2014) that potentially allow to check the plausibility of large scale soil loss assessments.

Code and data availability. The study was performed using openly available primary input data. For some of these data we do not have the
30 permission for further distribution. All input data can, however, be acquired from the rights holders of these data sets. All intermediate and final data that were generated in this study and the corresponding R code to manage and process the data are available upon request to the corresponding authors.

Author contributions. CS and MH designed the study and acquired and processed the input data. CS performed all analyses. MH and CS prepared the figures. KS and JK contributed in the methodological framework. CS, MH, BM, JK, and KS compiled the manuscript.

Competing interests. The authors declare that they have no conflict of interest.

Acknowledgements. This study was conducted within the frame of the Appear Project 158: *Capacity building on the water-energy-food*
5 *security Nexus through research and training in Kenya and Uganda (CapNex)* funded by the Austrian Partnership Programme in Higher Education and Research for Development (Appear). APPEAR is a programme of the Austrian Development Cooperation. The open-access publishing was supported by the BOKU Vienna Open Access Publishing Fund.

References

Alewell, C., Borrelli, P., Meusburger, K., and Panagos, P.: Using the USLE: Chances, challenges and limitations of soil erosion modelling, International Soil and Water Conservation Research, 7, 203 – 225, https://doi.org/https://doi.org/10.1016/j.iswcr.2019.05.004, 2019.

Angima, S. D., Stott, D. E., O'Neill, M. K., Ong, C. K., and Weesies, G. A.: Soil erosion prediction using RUSLE for central Kenyan highland conditions, Agriculture, Ecosystems and Environment, 97, 295–308, https://doi.org/10.1016/S0167-8809(03)00011-2, 2003.

Bai, Z. G., Dent, D. L., Olsson, L., and Schaepman, M. E.: Proxy global assessment of land degradation, Soil Use and Management, 24, 223–234, https://doi.org/10.1111/j.1475-2743.2008.00169.x, 2008.

Bamutaze, Y.: Patterns of water erosion and sediment loading in Manafwa in catchment on Mt. Elgon, Eastern Uganda, Ph.D. thesis, Department of Geography, Geo-information and Climatic Science, Makerere University, Kampala, Uganda, 2010.

Bamutaze, Y.: Revisiting socio-ecological resilience and sustainability in the coupled mountain landscapes in Eastern Africa, Current Opinion in Environmental Sustainability, 14, 257–265, https://doi.org/10.1016/j.cosust.2015.06.010, 2015.

Benavidez, R., Jackson, B., Maxwell, D., and Norton, K.: A review of the (Revised) Universal Soil Loss Equation ((R)USLE): with a view to increasing its global applicability and improving soil loss estimates, Hydrology and Earth System Sciences, 22, 6059–6086, https://doi.org/10.5194/hess-22-6059-2018, 2018.

Beven, K. and Young, P.: A guide to good practice in modeling semantics for authors and referees, Water Resources Research, 49, 5092–5098, https://doi.org/10.1002/wrcr.20393, 2013.

Beven, K. J.: On hypothesis testing in hydrology: Why falsification of models is still a really good idea, Wiley Interdisciplinary Reviews: Water, 5, e1278, https://doi.org/10.1002/wat2.1278, 2018.

Beven, K. J. and Brazier, R. E.: Dealing with Uncertainty in Erosion Model Predictions, in: Handbook of Erosion Modelling, edited by Morgan, R. P. C. and Nearing, M. A., chap. 4, pp. 52–79, Wiley Online Library, 2011.

Bivand, R., Keitt, T., and Rowlingson, B.: rgdal: Bindings for the 'Geospatial' Data Abstraction Library, https://CRAN.R-project.org/package=rgdal, r package version 1.4-3, 2019.

Blanco-Canqui, H. and Lal, R.: Principles of soil conservation and management, Springer Science & Business Media, 2008.

Boardman, J.: Soil erosion by water: problems and prospects for research, in: Advances in Hillslope Processes, edited by Anderson, M. G. and Brooks, S. M., pp. 489–505, Wiley, Chichester, UK, 1996.

Boardman, J.: Soil erosion science: Reflections on the limitations of current approaches, CATENA, 68, 73–86, https://doi.org/10.1016/j.catena.2006.03.007, 2006.

Bollinnne, A.: Adjusting the universal soil loss equation to use in Western Europe, in: Soil Erosion and Conservation, edited by El-Swaify, S., Moldenhauer, W., and A., L., pp. 206–213, Soil Conservation Society of America, Ankeny, Iowa, 1985.

Borrelli, P., Robinson, D. A., Fleischer, L. R., Lugato, E., Ballabio, C., Alewell, C., Meusburger, K., Modugno, S., Schütt, B., Ferro, V., Bagarello, V., Oost, K. V., Montanarella, L., and Panagos, P.: An assessment of the global impact of 21st century land use change on soil erosion, Nature Communications, 8, https://doi.org/10.1038/s41467-017-02142-7, 2017.

Bosco, C., Rigo, D. D., and Dewitte, O.: Visual Validation of the e-RUSLE Model Applied at the Pan-European Scale, Scientific Topics Focus 1, https://doi.org/10.6084/m9.figshare.844627.v5, MRI-11a13. Notes on Transdisciplinary Modelling for Environment, Maieutike Research Initiative, 2014.

Bosco, C., De Rigo, D., Dewitte, O., Poesen, J., and Panagos, P.: Modelling soil erosion at European scale: Towards harmonization and reproducibility, Natural Hazards and Earth System Sciences, 15, 225–245, https://doi.org/10.5194/nhess-15-225-2015, 2015.

Browning, G. M., Parish, C. L., and Glass, J. A.: A method for determining the use of limitations of rotation and conservation practices in the control of soil erosion in Iowa, Journal of the American Society of Agronomy, 39, 65–73, 1947.

Böhner, J. and Selige, T.: Spatial Prediction of Soil Attributes Using Terrain Analysis and Climate Regionalisation, in: 'SAGA - Analysis and Modelling Applications', edited by Böhner, J., McCloy, K., and Strobl, J., Göttinger Geographische Abhandlungen, Göttingen, 13-28, 2006.

Carroll, M., Townshend, J., DiMiceli, C., Noojipady, P., and Sohlberg, R.: A new global raster water mask at 250 m resolution, International Journal of Digital Earth, 2, 291–308, https://doi.org/10.1080/17538940902951401, 2009.

Channan, S., Collins, K., and Emanuel, W. R.: Global mosaics of the standard MODIS land cover type data, 2014.

Conrad, O., Bechtel, B., Bock, M., Dietrich, H., Fischer, E., Gerlitz, L., Wehberg, J., Wichmann, V., and Böhner, J.: System for Automated Geoscientific Analyses (SAGA) v. 2.1.4, Geoscientific Model Development, 8, 1991–2007, https://doi.org/10.5194/gmd-8-1991-2015, 2015.

De Meyer, A., Poesen, J., Isabirye, M., Deckers, J., and Raes, D.: Soil erosion rates in tropical villages: A case study from Lake Victoria Basin, Uganda, CATENA, 84, 89 – 98, https://doi.org/10.1016/j.catena.2010.10.001, 2011.

Desmet, P. and Govers, G.: A GIS procedure for automatically calculating the USLE LS factor on topographically complex landscape units, Journal of soil and water conservation, 51, 427–433, 1996.

Didan, K.: MOD13Q1 MODIS/Terra vegetation indices 16-day L3 global 250m SIN grid V006, NASA EOSDIS Land Processes DAAC, https://doi.org/10.5067/MODIS/MOD13Q1.006, 2015.

Dissmeyer, G. and Foster, G.: A guide for predicting sheet and rill erosion on forest land, Technical Publication SA-TP-11, USDA Forest Service-State and Private Forestry Southeastern Area, 1980.

Ebisemiju, F.: Gully morphometric controls in a laterite terrain, Guyana, Geo Eco Trop, 12, 41–59, 1988.

ESA: ESA Land Cover Climate Change Initiative (ESA LC CCI) data: ESACCI-LC-L4-LCCS-Map-300m-P1Y-1992_2015-v2.0.7.tif via Centre for Environmental Data Analysis, http://maps.elie.ucl.ac.be/CCI, 2017.

ESRI: ArcGIS Desktop: Release 10.1, 2012.

Evans, R.: Some methods of directly assessing water erosion of cultivated land - a comparison of measurements made on plots and in fields, Progress in Physical Geography, 19, 115–129, https://doi.org/10.1177/030913339501900106, 1995.

Evans, R.: An alternative way to assess water erosion of cultivated land – field-based measurements: and analysis of some results, Applied Geography, 22, 187–207, https://doi.org/10.1016/s0143-6228(02)00004-8, 2002.

Evans, R.: Assessment and monitoring of accelerated water erosion of cultivated land - when will reality be acknowledged?, Soil Use and Management, 29, 105–118, https://doi.org/10.1111/sum.12010, 2013.

Evans, R. and Boardman, J.: The new assessment of soil loss by water erosion in Europe. Panagos P. et al., 2015 Environmental Science & Policy 54, 438–447—A response, Environmental Science & Policy, 58, 11–15, https://doi.org/10.1016/j.envsci.2015.12.013, 2016a.

Evans, R. and Boardman, J.: A reply to panagos et al., 2016 (Environmental science & policy 59 (2016) 53–57, Environmental science & policy, 60, 63–68, https://doi.org/10.1016/j.envsci.2016.03.004, 2016b.

FAO-PNUMA-UNESCO: Metodología provisional para la evaluación de la degradación de los suelos, Tech. rep., Organización de las Naciones Unidas para el Desarrollo de la Agricultura y la Alimentación (FAO), Programa de las Naciones Unidas para el Medio Ambiente (PNUMA), Organización de las Naciones para el Medio Ambiente (UNESCO), Roma, Italia (In Spanish), 1980.

Favis-Mortlock, D.: Validation of Field-Scale Soil Erosion Models Using Common Datasets, in: Modelling Soil Erosion by Water, NATO ASI Series book series (volume 55), edited by Boardman, J. and Favis-Mortlock, D., chap. 9, pp. 89–127, Springer Berlin Heidelberg, https://doi.org/10.1007/978-3-642-58913-3_9, 1998.

Fick, S. E. and Hijmans, R. J.: WorldClim 2: new 1-km spatial resolution climate surfaces for global land areas, International Journal of Climatology, 37, 4302–4315, https://doi.org/10.1002/joc.5086, 2017.

Friedl, M. A., Sulla-Menashe, D., Tan, B., Schneider, A., Ramankutty, N., Sibley, A., and Huang, X.: MODIS Collection 5 global land cover: Algorithm refinements and characterization of new datasets, 2001-2012, Collection 5.1 IGBP Land Cover, http://glcf.umd.edu/data/lc/, 2010.

García-Ruiz, J. M., Beguería, S., Nadal-Romero, E., González-Hidalgo, J. C., Lana-Renault, N., and Sanjuán, Y.: A meta-analysis of soil erosion rates across the world, Geomorphology, 239, 160 – 173, https://doi.org/10.1016/j.geomorph.2015.03.008, 2015.

Govers, G.: Misapplications and Misconceptions of Erosion Models, in: Handbook of Erosion Modelling, edited by Morgan, R. P. C. and Nearing, M. A., chap. 7, pp. 117–134, Blackwell Publishing Ltd., 2011.

Grolemund, G. and Wickham, H.: Dates and Times Made Easy with lubridate, Journal of Statistical Software, 40, 1–25, https://doi.org/10.18637/jss.v040.i03, 2011.

Hengl, T., De Jesus, J. M., Heuvelink, G. B., Gonzalez, M. R., Kilibarda, M., Blagotić, A., Shangguan, W., Wright, M. N., Geng, X., Bauer-Marschallinger, B., Guevara, M. A., Vargas, R., MacMillan, R. A., Batjes, N. H., Leenaars, J. G., Ribeiro, E., Wheeler, I., Mantel, S., and Kempen, B.: SoilGrids250m: Global gridded soil information based on machine learning, PLoS ONE, 12, 1–40, https://doi.org/10.1371/journal.pone.0169748, 2017.

Henry, L. and Wickham, H.: purrr: Functional Programming Tools, https://CRAN.R-project.org/package=purrr, r package version 0.3.2, 2019.

Hernando, D. and Romana, M. G.: Development of a Soil Erosion Classification System for Cut and Fill Slopes, Transportation Infrastructure Geotechnology, 2, 155–166, https://doi.org/10.1007/s40515-015-0024-9, 2015.

Hijmans, R. J.: raster: Geographic Data Analysis and Modeling, https://CRAN.R-project.org/package=raster, r package version 2.9-5, 2019.

Huffman, G. J., Bolvin, D. T., Nelkin, E. J., Wolff, D. B., Adler, R. F., Gu, G., Hong, Y., Bowman, K. P., and Stocker, E. F.: The TRMM Multisatellite Precipitation Analysis (TMPA): Quasi-Global, Multiyear, Combined-Sensor Precipitation Estimates at Fine Scales, Journal of Hydrometeorology, 8, 38–55, https://doi.org/10.1175/jhm560.1, 2007.

Jarvis, A., Reuter, H. I., Nelson, A., and Guevara, E.: Hole-filled SRTM for the globe Version 4, https://cgiarcsi.community/data/srtm-90m-digital-elevation-database-v4-1/, available from the CGIAR-CSI SRTM 90m Database, 2008.

Jetten, V. and Favis-Mortlock, D.: Modelling Soil Erosion in Europe, in: Soil Erosion in Europe, edited by Boardman, J. and Poesen, J., chap. 50, pp. 695–716, John Wiley & Sons, Ltd, https://doi.org/10.1002/0470859202.ch50, 2006.

Jones, A., Breuning-Madsen, H., Brossard, M., Dampha, A., Deckers, J., Dewitte, O., Gallali, T., Hallett, S., Jones, R., Kilasara, M., Le Roux, P., Micheli, E., Spaargaren, O., Thombiano, L., Van Ranst, E., Yemefack, M., and Zougmoré, R., eds.: Soil Atlas of Africa, European Union Joint Research Centre, 2013.

Karamage, F., Zhang, C., Liu, T., Maganda, A., and Isabwe, A.: Soil erosion risk assessment in Uganda, Forests, 8, 52, https://doi.org/10.3390/f8020052, 2017.

Kinnell, P.: Event soil loss, runoff and the Universal Soil Loss Equation family of models: A review, Journal of Hydrology, 385, 384 – 397, https://doi.org/10.1016/j.jhydrol.2010.01.024, 2010.

Kithiia, S. M.: Land use changes and their effects on sediment transport and soil erosion within the Athi drainage basin, Kenya, in: Human Impact on Erosion and Sedimentation (Proceedings of Rabat Symposium 56, April 1997), IAHS Publ. no. 245, edited by Walling, D. E. and Probst, J.-L., pp. 145–150, International Association of Hydrological Sciences, 1997.

KNBS: Section agriculture, in: County Statistical Abstracts, Kenya National Bureau of Statistics, Nairobi, Kenya, 2015.

5   Lo, A., El-Swaify, S. A., Dangler, E. W., and Shinshiro, L.: Effectiveness of EI30 as an erosivity index in Hawaii, in: Soil Erosion and Conservation, edited by El-Swaify, S. A., Moldenhauer, W. C., and Lo, A., pp. 384–392, Soil Conservation Society of America, Ankeny, IA, USA, 1985.

LUCAS: Land Use/Cover Area Frame Statistical Survey Database, http://epp.eurostat.ec.europa.eu/portal/page/portal/lucas/data/LUCAS_ primary_data/2012, 2012.

10   Lufafa, A., Tenywa, M., Isabirye, M., Majaliwa, M., and Woomer, P.: Prediction of soil erosion in a Lake Victoria basin catchment using a GIS-based Universal Soil Loss model, Agricultural Systems, 76, 883–894, https://doi.org/10.1016/s0308-521x(02)00012-4, 2003.

Microsoft Corporation and Weston, S.: doSNOW: Foreach Parallel Adaptor for the 'snow' Package, https://CRAN.R-project.org/package= doSNOW, r package version 1.0.16, 2017a.

Microsoft Corporation and Weston, S.: foreach: Provides Foreach Looping Construct for R, https://CRAN.R-project.org/package=foreach, r
15   package version 1.4.4, 2017b.

Monfreda, C., Ramankutty, N., and Foley, J. A.: Farming the planet: 2. Geographic distribution of crop areas, yields, physiological types, and net primary production in the year 2000, Global Biogeochemical Cycles, 22, 1–19, https://doi.org/10.1029/2007GB002947, 2008.

Montgomery, D. R.: Soil erosion and agricultural sustainability, Proceedings of the National Academy of Sciences, 104, 13 268–13 272, https://doi.org/10.1073/pnas.0611508104, 2007.

20   Moore, I. D., Grayson, R. B., and Ladson, A. R.: Digital terrain modelling: A review of hydrological, geomorphological, and biological applications, Hydrological Processes, 5, 3–30, https://doi.org/10.1002/hyp.3360050103, 1991.

Moore, T. R.: Rainfall Erosivity in East Africa, Geografiska Annaler. Series A, Physical Geography, 61, 147–156, https://doi.org/10.2307/520909, 1979.

Morgan, R. P. C.: Soil erosion and conservation, John Wiley & Sons, 2009.

25   Musgrave, G. W.: The quantitative evaluation of factors in water erosion, a first approximation, Journal of Soil and Water Conservation, 2, 133–138, 1947.

Müller, K. and Wickham, H.: tibble: Simple Data Frames, https://CRAN.R-project.org/package=tibble, r package version 2.1.3, 2019.

Müller, K., Wickham, H., James, D. A., and Falcon, S.: RSQLite: 'SQLite' Interface for R, https://CRAN.R-project.org/package=RSQLite, r package version 2.1.1, 2018.

30   Naipal, V., Reick, C., Pongratz, J., and Van Oost, K.: Improving the global applicability of the RUSLE model - Adjustment of the topographical and rainfall erosivity factors, Geoscientific Model Development, 8, 2893–2913, https://doi.org/10.5194/gmd-8-2893-2015, 2015.

Nakil, M.: Analysis of parameters causing water induced soil erosion, in: Unpublished Fifth Annual Progress Seminar, Indian Institute of Technology, Bombay, 2014.

NASA/METI/AIST/Japan Spacesystems, and U.S./Japan ASTER Science Team: ASTER Global Digital Elevation Model,
35   https://doi.org/10.5067/ASTER/ASTGTM.002, 2009.

Olivares, R. U., Bulos, A. D. M., and Sombrito, E. Z.: Environmental assessment of soil erosion in Inabanga watershed (Bohol, Philippines), Energy, Ecology and Environment, 1, 98–108, https://doi.org/10.1007/s40974-016-0012-0, 2016.

Panagos, P., Meusburger, K., Ballabio, C., Borrelli, P., and Alewell, C.: Soil erodibility in Europe: A high-resolution dataset based on LUCAS, Science of the Total Environment, 479-480, 189–200, https://doi.org/10.1016/j.scitotenv.2014.02.010, 2014.

Panagos, P., Ballabio, C., Borrelli, P., Meusburger, K., Klik, A., Rousseva, S., Tadić, M. P., Michaelides, S., Hrabalíková, M., Olsen, P., Aalto, J., Lakatos, M., Rymszewicz, A., Dumitrescu, A., Beguería, S., and Alewell, C.: Rainfall erosivity in Europe, Science of the Total Environment, 511, 801–814, https://doi.org/10.1016/j.scitotenv.2015.01.008, 2015a.

Panagos, P., Borrelli, P., and Meusburger, K.: A New European Slope Length and Steepness Factor (LS-Factor) for Modeling Soil Erosion by Water, Geosciences, 5, 117–126, https://doi.org/10.3390/geosciences5020117, 2015b.

Panagos, P., Borrelli, P., Meusburger, K., Alewell, C., Lugato, E., and Montanarella, L.: Estimating the soil erosion cover-management factor at the European scale, Land Use Policy, 48, 38–50, https://doi.org/10.1016/j.landusepol.2015.05.021, 2015c.

Panagos, P., Borrelli, P., Meusburger, K., van der Zanden, E. H., Poesen, J., and Alewell, C.: Modelling the effect of support practices (P-factor) on the reduction of soil erosion by water at European scale, Environmental Science and Policy, 51, 23–34, https://doi.org/10.1016/j.envsci.2015.03.012, 2015d.

Panagos, P., Borrelli, P., Poesen, J., Ballabio, C., Lugato, E., Meusburger, K., Montanarella, L., and Alewell, C.: The new assessment of soil loss by water erosion in Europe, Environmental Science and Policy, 54, 438–447, https://doi.org/10.1016/j.envsci.2015.08.012, 2015e.

Panagos, P., Borrelli, P., Poesen, J., Meusburger, K., Ballabio, C., Lugato, E., Montanarella, L., and Alewell, C.: Reply to "The new assessment of soil loss by water erosion in Europe. Panagos P. et al., 2015 Environ. Sci. Policy 54, 438–447—A response" by Evans and Boardman [Environ. Sci. Policy 58, 11–15], Environmental Science & Policy, 59, 53–57, https://doi.org/10.1016/j.envsci.2016.02.010, 2016.

Panagos, P., Borrelli, P., Meusburger, K., Yu, B., Klik, A., Jae Lim, K., Yang, J. E., Ni, J., Miao, C., Chattopadhyay, N., Sadeghi, S. H., Hazbavi, Z., Zabihi, M., Larionov, G. A., Krasnov, S. F., Gorobets, A. V., Levi, Y., Erpul, G., Birkel, C., Hoyos, N., Naipal, V., Oliveira, P. T. S., Bonilla, C. A., Meddi, M., Nel, W., Al Dashti, H., Boni, M., Diodato, N., Van Oost, K., Nearing, M., and Ballabio, C.: Global rainfall erosivity assessment based on high-temporal resolution rainfall records, Scientific Reports, 7, 4175, https://doi.org/10.1038/s41598-017-04282-8, 2017.

Pebesma, E.: Simple Features for R: Standardized Support for Spatial Vector Data, The R Journal, 10, 439–446, https://doi.org/10.32614/RJ-2018-009, 2018.

Prasuhn, V., Liniger, H., Gisler, S., Herweg, K., Candinas, A., and Clément, J.-P.: A high-resolution soil erosion risk map of Switzerland as strategic policy support system, Land Use Policy, 32, 281–291, https://doi.org/10.1016/j.landusepol.2012.11.006, 2013.

R Core Team: R: A language and environment for statistical computing., https://www.r-project.org/, 2019.

Renard, K. G. and Freimund, J. R.: Using monthly precipitation data to estimate the R-factor in the revised USLE, Journal of Hydrology, 157, 287–306, https://doi.org/10.1016/0022-1694(94)90110-4, 1994.

Renard, K. G., Foster, G. R., Weesies, G. A., and Porter, J. P.: RUSLE: Revised universal soil loss equation, Journal of Soil and Water Conservation, 46, 30–33, 1991.

Renard, K. G., Foster, G. R., Weesies, G., McCool, D., and Yoder, D.: Predicting soil erosion by water: a guide to conservation planning with the Revised Universal Soil Loss Equation (RUSLE), U.S. Department of Agriculture, Agriculture Handbook No.703, Washington, DC, 1997.

Renard, K. G., Yoder, D. C., Lightle, D. T., and Dabney, S. M.: Univeral Soil Loss Equation and Revised Universal Soil Loss Equation, in: Handbook of Erosion Modelling, edited by Morgan, R. P. C. and Nearing, M. A., chap. 8, pp. 137–167, Wiley Online Library, 2011.

Risse, L. M., Nearing, M. A., Laflen, J. M., and Nicks, A. D.: Error Assessment in the Universal Soil Loss Equation, Soil Science Society of America Journal, 57, 825, https://doi.org/10.2136/sssaj1993.03615995005700030032x, 1993.

Roose, E. J.: Erosion et ruissellement en Afrique de l'Ouest : vingt années de mesures en petites parcelles expérimentales, Tech. rep., Office de la scientifique et Technique Outre-Mer, Centre D'Adiopodoumé, Côte d'Ivoire, 1975.

5 Ross, N.: fasterize: Fast Polygon to Raster Conversion, https://CRAN.R-project.org/package=fasterize, r package version 1.0.0, 2018.

Shangguan, W., Dai, Y., Duan, Q., Liu, B., and Yuan, H.: A global soil data set for earth system modeling, Journal of Advances in Modeling Earth Systems, 6, 249–263, https://doi.org/10.1002/2013MS000293, 2014.

Smith, D. D.: Interpretation of soil conservation data for field use, Agricultural Engineering, 22, 173–175, 1941.

Spaeth, K. E., Pierson, F. B., Weltz, M. A., and Blackburn, W. H.: Evaluation of USLE and RUSLE Estimated Soil Loss on Rangeland, Journal of Range Management, 56, 234–246, https://doi.org/10.2307/4003812, 2003.

10 Sutherland, R. A. and Bryan, K. B.: Runoff and erosion from a small semiarid catchment, Baringo district, Kenya, Applied Geography, 10, 91 – 109, https://doi.org/10.1016/0143-6228(90)90046-R, 1990.

Tamene, L. and Le, Q. B.: Estimating soil erosion in sub-Saharan Africa based on landscape similarity mapping and using the revised universal soil loss equation (RUSLE), Nutrient Cycling in Agroecosystems, 102, 17–31, https://doi.org/10.1007/s10705-015-9674-9, 2015.

15 Tiwari, A. K., Risse, L. M., and Nearing, M. A.: Evaluation of WEPP and its comparison with USLE and RUSLE, Transactions of the ASAE, 43, 1129–1135, https://doi.org/10.13031/2013.3005, 2000.

Torri, D., Poesen, J. W. A., and Borselli, L.: Predictability and uncertainty of the soil erodibility factor using a global dataset, CATENA, 31, 1–22, https://doi.org/https://doi.org/10.1016/S0341-8162(97)00036-2, 1997.

UBOS: Volume IV: Crop Area and Production Report, in: Uganda Census of Agriculture 2008/2009, p. 178, Uganda Bureau of Statistics, Kampala, Uganda, 2010.

20 Van-Camp, L., Bujarrabal, B., Gentile, A. R., Jones, R. J., Montanarella, L., Olazabal, C., and Selvaradjou, S.-K.: Reports of the Technical Working Groups Established under the Thematic Strategy for Soil Protection. EUR 21319 EN/6, 872 pp., Tech. rep., Office for Official Publications of the European Communities, Luxembourg, 2004.

Van der Knijff, J., Jones, R., and Montanarella, L.: Soil Erosion Risk Assessment in Europe, EUR 19044 EN., Tech. rep., European Soil Bureau, European Comission, 2000.

25 Vrieling, A., Sterk, G., and de Jong, S. M.: Satellite-based estimation of rainfall erosivity for Africa, Journal of Hydrology, 395, 235–241, https://doi.org/10.1016/j.jhydrol.2010.10.035, 2010.

Vrieling, A., Hoedjes, J. C. B., and van der Velde, M.: Towards large-scale monitoring of soil erosion in Africa: Accounting for the dynamics of rainfall erosivity, Global and Planetary Change, 115, 33–43, https://doi.org/10.1016/j.gloplacha.2014.01.009, 2014.

30 Warren, S. D., Mitasova, H., Hohmann, M. G., Landsberger, S., Iskander, F. Y., Ruzycki, T. S., and Senseman, G. M.: Validation of a 3-D enhancement of the Universal Soil Loss Equation for prediction of soil erosion and sediment deposition, CATENA, 64, 281–296, https://doi.org/10.1016/j.catena.2005.08.010, 2005.

Weltz, M. A., Kidwell, M. R., and Fox, H. D.: Influence of abiotic and biotic factors in measuring and modeling soil erosion on rangelands: state of knowledge., Rangeland Ecology & Management/Journal of Range Management Archives, 51, 482–495, 1998.

35 Wickham, H.: forcats: Tools for Working with Categorical Variables (Factors), https://CRAN.R-project.org/package=forcats, r package version 0.4.0, 2019.

Wickham, H. and Henry, L.: tidyr: Easily Tidy Data with 'spread()' and 'gather()' Functions, https://CRAN.R-project.org/package=tidyr, r package version 0.8.3, 2019.

Wickham, H. and Ruiz, E.: dbplyr: A 'dplyr' Back End for Databases, https://CRAN.R-project.org/package=dbplyr, r package version 1.4.0, 2019.

Wickham, H., Chang, W., Henry, L., Pedersen, T. L., Takahashi, K., Wilke, C., Woo, K., and Yutani, H.: ggplot2: Create Elegant Data Visualisations Using the Grammar of Graphics, http://ggplot2.tidyverse.org, r package version 3.1.1, 2019a.

5 Wickham, H., François, R., Henry, L., and Müller, K.: dplyr: A Grammar of Data Manipulation, https://CRAN.R-project.org/package=dplyr, r package version 0.8.1, 2019b.

Williams, J. R.: The EPIC model - Soil Erosion, in: Computer Models of Watershed Hydrology, edited by Singh, V. P., pp. 909–1000, Water Resources Publications, Highlands Ranch, CO, USA, 1995.

Wischmeier, W. H. and Smith, D. D.: Predicting rainfall-erosion losses from cropland east of the Rocky Mountains., U.S. Department of
10   Agriculture, Agricultural Handbook No. 282, Washington, DC, 1965.

Wischmeier, W. H. and Smith, D. D.: Predicting rainfall erosion losses - a guide to conservation planning., U.S. Department of Agriculture, Agricultural Handbook No. 537, Hyattsville, Maryland, 1987.

Yang, D., Kanae, S., Oki, T., Koike, T., and Musiake, K.: Global potential soil erosion with reference to land use and climate changes, Hydrological Processes, 17, 2913–2928, https://doi.org/10.1002/hyp.1441, 2003.

15 Young, P. C.: Data-based Mechanistic Modelling and Validation of Rainfall-Flow Processes, in: Model Validation: Perspectives in Hydrological Science, edited by Anderson, M. G. and Bates, P., pp. 117–161, John Wiley, Chichester, 2001.

Zachar, D.: Soil Erosion (Developments in Soil Science 10), Elsevier Scientific Publishing Company, Amsterdam, 1982.

Zingg, A. W.: Degree and length of land slope as it affects soil loss in run-off., Agricultural Engineering, 21, 59–64, 1940.